

Pressure-induced silicon coordination and tetrahedral structural changes in alkali oxide–silica melts up to 12 GPa: NMR, Raman, and infrared spectroscopy

XIANYU XUE*

C. M. Scarfe Laboratory of Experimental Petrology, Department of Geology and Institute of Earth and Planetary Physics,
University of Alberta, Edmonton T6G 2E3, Canada

JONATHAN F. STEBBINS

Department of Geology, Stanford University, Stanford, California 94305, U.S.A.

MASAMI KANZAKI**

C. M. Scarfe Laboratory of Experimental Petrology, Department of Geology and Institute of Earth and Planetary Physics,
University of Alberta, Edmonton T6G 2E3, Canada

PAUL F. McMILLAN, BRENT POE

Department of Chemistry, Arizona State University, Tempe, Arizona 85287, U.S.A.

ABSTRACT

The ^{29}Si and ^{23}Na NMR, Raman, and infrared spectra of glasses quenched from liquids at pressures up to 12 GPa for three alkali silicate compositions ($\text{Na}_2\text{Si}_2\text{O}_5$, $\text{Na}_2\text{Si}_4\text{O}_9$, $\text{K}_2\text{Si}_4\text{O}_9$) and silica (SiO_2) reveal systematic changes in the melt structure with pressure. The most novel change is the occurrence of ^{15}Si and ^{16}Si species at high pressures identified by peaks in the ^{29}Si MAS NMR spectra of the alkali silicate glasses. The abundances of both ^{15}Si and ^{16}Si increase with pressure. At a given pressure there are more such species in the $\text{Na}_2\text{Si}_4\text{O}_9$ composition than in $\text{Na}_2\text{Si}_2\text{O}_5$ composition. These species are not observed in a SiO_2 glass quenched at 6 GPa. The occurrence of these highly coordinated Si species is consistent with changes in the Raman and infrared spectra of the alkali silicate glasses, although the peak assignments in these spectra are not unique. The change in Si coordination with pressure and composition in these compositions can be accounted for by a model in which ^{15}Si and ^{16}Si form at the expense of nonbridging O atoms. This model may be generalized to all partially depolymerized melts. Changes in the tetrahedral structure with increasing pressure include Q speciation disproportionation, reduction of mean Si–O–Si angle, and development of new ^{14}Si species that share O with ^{15}Si or ^{16}Si . The observed structural changes have implications for the physical and thermodynamic properties of silicate melts. ^{15}Si has been previously envisaged as a transient state for the viscous flow and diffusion processes in silicate melts. The occurrence of ^{15}Si in the high pressure glasses suggests that ^{15}Si represents a local energy minimum and its stabilization may partly account for the enhancement of these dynamic processes. Increased configurational entropy as a result of greater distribution of Si coordinations and Q species at high pressures could also contribute to the reduced melt viscosity.

INTRODUCTION

A knowledge of the structure of silicate melts and its relationship to their physical and chemical properties at high pressures is necessary in order to understand magmatic processes. It is well known that the local structure of silicate melts and glasses at ambient pressure is characterized by a regular coordination of Si by four O atoms (^{4}Si) as in crystalline silicates. The longer range structure of silicate melts, although not well understood, has been

described as a mixture of a restricted variety of structure units (e.g., Mysen, 1988; McMillan, 1984; Stebbins and Farnan, 1989). The connectivity of SiO_4 tetrahedra, denoted as Q^n species (SiO_4 tetrahedra with n nearest SiO_4 or AlO_4 neighbors) is an important parameter describing this intermediate order.

It has been predicted from molecular dynamic simulations that Si coordination increases in silicate melts with increasing pressure (e.g., Angell et al., 1982, 1983, 1987, 1988; Matsui et al., 1982; Matsui and Kawamura, 1980, 1984), analogous to that observed in crystalline silicates (see compilation in Liu and Bassett, 1986). Direct in situ spectroscopic study of silicate melt structure at combined high pressures and high temperatures is difficult, however, because of the limitations of spectroscopic tech-

* Present address: Department of Geology, Stanford University, Stanford, California 94305, U.S.A.

** Present address: Department of Inorganic Materials, Tokyo Institute of Technology, O-okayama, Meguro-ku, Tokyo 152, Japan.

niques and high pressure apparatus. Information concerning high pressure melt structure has mostly been obtained indirectly either by in situ spectroscopic measurements on glasses densified at room temperature in a diamond anvil cell (e.g., Hemley et al., 1986; Williams and Jeanloz, 1988; Itie et al., 1989; Wolf et al., 1990), or by studies at room temperature and pressure of glasses quenched from liquids at high pressures with a piston-cylinder or multianvil apparatus (e.g., Mysen et al., 1983; Fleet et al., 1984; Hochella and Brown, 1985; Ohtani et al., 1985; Xue et al., 1989; Stebbins and McMillan, 1989).

Hemley et al. (1986) interpreted in situ Raman spectra of SiO_2 glasses up to 27 GPa at room temperature as indicating a change in the Si-O-Si angle distribution below 8 GPa and a reduction of ring size between 8 and 30 GPa, but there is no clear indication of a change in the Si coordination. Williams and Jeanloz (1988), on the other hand, suggested that in situ infrared absorption spectra on SiO_2 , $\text{CaAl}_2\text{Si}_2\text{O}_8$, and $\text{CaMgSi}_2\text{O}_6$ glasses at room temperature and pressures up to 40 GPa indicate the formation of species with higher coordinations above 20 GPa. Recently, Itie et al. (1989) reported in situ X-ray absorption near-edge structure (XANES) and extended X-ray absorption fine structure (EXAFS) data for amorphous GeO_2 up to 30 GPa at room temperature which suggests changes in average Ge-O bond lengths consistent with a transformation of Ge from fourfold to sixfold coordination at 7–9 GPa. However, liquids may have additional mechanisms of structural adjustments with pressure compared to glasses at room temperature because the much higher thermal energy of liquids may allow atomic motions to overcome potential barriers for more dramatic structural changes.

Spectroscopic studies of silicate glasses quenched from liquids at high pressures complement the in situ spectroscopic studies of room temperature densified glasses. It is generally assumed that the structure of a quenched glass represents that of the liquid at its glass transition temperature (T_g) (e.g., Gibbs and DiMarzio, 1958), although some local structural adjustments may occur during decompression. Most of this type of work was limited to tectosilicate compositions and to pressures below 4 GPa (using a piston-cylinder apparatus). These studies revealed no Si or Al coordination change with pressure (e.g., Mysen et al., 1983; Fleet et al., 1984; Hochella and Brown, 1985). However, it is necessary to extend such work to less polymerized systems and to higher pressures. The multianvil press is particularly useful for this purpose because it can generate stable high temperatures above 2000 °C and high pressures up to 25 GPa (Ito et al., 1984). Both piston-cylinder and multianvil apparatus can produce samples that are large enough for the use of MAS NMR (magic angle spinning nuclear magnetic resonance spectroscopy). With this approach, Ohtani et al. (1985) first suggested a pressure-induced coordination change of Al from fourfold to sixfold in $\text{NaAlSi}_3\text{O}_8$ (albite) glasses at 6–8 GPa. However, quantification of these results is difficult because of the nuclear quadrupolar moment of

^{27}Al , and a recent study by Stebbins and Sykes (1990) questioned some of those conclusions. Solid-state ^{29}Si MAS NMR, on the other hand, is unique in identifying and quantifying Si of different coordinations in amorphous materials, and can also provide information concerning the intermediate-range structure (e.g., Dupree et al., 1987; Kirkpatrick, 1988; Stebbins, 1987). We recently applied the ^{29}Si MAS NMR technique to investigate the structure of alkali silicate melts at high pressures. In our reports on $\text{Na}_2\text{Si}_2\text{O}_5$ and $\text{K}_2\text{Si}_4\text{O}_9$ glasses quenched from liquids (Xue et al., 1989; Stebbins and McMillan, 1989), we presented evidence for pressure-induced five-coordinated Si (^{5}Si) and six-coordinated Si (^{6}Si) species in these glasses. We also documented changes in the Si tetrahedral structure that, at least for $\text{Na}_2\text{Si}_2\text{O}_5$ glasses, can be described as greater Q speciation disproportionation at high pressures. These results suggest that changes in both Si coordination and tetrahedral structure are important during compression of silicate liquids over a large pressure interval.

The study reported here was aimed at further investigating the systematic changes in Si coordinations and tetrahedral structures of silicate melts with pressure and composition and at gaining an insight into the mechanism of these changes. Toward this goal, we have further quantified our previous ^{29}Si NMR results for $\text{Na}_2\text{Si}_2\text{O}_5$ glasses and obtained new ^{29}Si NMR spectra for $\text{Na}_2\text{Si}_4\text{O}_9$ glasses quenched at pressures up to 12 GPa, $\text{K}_2\text{Si}_4\text{O}_9$ glasses quenched at 4 and 6 GPa, and a SiO_2 glass quenched at 6 GPa. These compositional series provide a glimpse of the structural dependence of silicate melts on both the degree of polymerization (characterized by nonbridging O atoms per tetrahedrally coordinated cation; NBO/T) and on the size of the network modifying cations at high pressures. We have also obtained ^{23}Na NMR, Raman, and infrared spectra for the same samples, as well as Raman and infrared spectra for a $\text{Na}_2\text{Si}_2\text{O}_5$ glass quenched at 10 GPa and $\text{K}_2\text{Si}_4\text{O}_9$ glasses quenched at pressures up to 8 GPa.

EXPERIMENTAL METHODS

Sample syntheses

We described the procedures for the preparation of starting ^{29}Si enriched $\text{Na}_2\text{Si}_2\text{O}_5$ and $\text{K}_2\text{Si}_4\text{O}_9$ glasses previously (Xue et al., 1989; Stebbins and McMillan, 1989). We prepared the ^{29}Si enriched $\text{Na}_2\text{Si}_4\text{O}_9$ starting glass in a similar way by fusion at 1200 °C of Na_2CO_3 and ^{29}Si -enriched (95%) SiO_2 (Oak Ridge National Laboratory) with 0.2 wt% Gd_2O_3 to shorten the spin-lattice relaxation time. We did not chemically analyze these samples because of their small size and the expense of the ^{29}Si enriched material. However, both the NMR and Raman spectra are essentially identical to previously published results for analyzed samples, indicating close to nominal silica contents. The starting material used for the study of SiO_2 glass was ^{29}Si enriched (95%) SiO_2 (cristobalite) with 0.2 wt% Gd_2O_3 . For some Raman and infrared mea-

surements, we used the NBS standard $\text{Na}_2\text{Si}_2\text{O}_5$ glass or a $\text{K}_2\text{Si}_4\text{O}_9$ glass sample with a normal Si isotopic composition as starting material. We prepared the latter by decarbonization of dried K_2CO_3 and SiO_2 powders at 700 °C for 3 d and subsequent melting at 1100 °C for 2 h. Optical examination and back scattered electron image both confirm that the glass obtained was homogeneous. Electron microprobe analysis reveals that the glass was stoichiometric [72.5 (0.4) wt% SiO_2].

We synthesized the glass samples quenched at pressures <4 GPa in a piston-cylinder apparatus at Arizona State University as described previously (Stebbins and McMillan, 1989; Dickinson et al., 1990). We produced the glass samples quenched at pressures ≥ 4 GPa in a USSA-2000 multianvil press at the University of Alberta. For the alkali silicate compositions, we loaded about 10 mg of glass powder in a Pt tube (with one end sealed), then dried it in an oven at 110 °C before sealing the top of the tube. For the SiO_2 sample, we used Re foil as capsule material because of its high melting temperature. We dehydrated the furnace assembly at 1000 °C for about 1 h just before the experiment. We determined the liquidus temperatures for all compositions by separate experiments (alkali silicates: Kanzaki et al., 1989; SiO_2 : Kanzaki, 1991). In a typical experiment, we first compressed the sample to the desired pressure, then heated it to above the liquidus temperature and held it at the desired temperature, 10–20 min for the alkali silicates and 1–2 min for SiO_2 , before isobarically quenching it by cutting the power. Temperature dropped to 400 °C within about 2 s. The rate of subsequent decompression was 2–3 GPa/h. Temperature and pressure control were automated via a Eurotherm controller and a personal computer respectively. The upper pressure limit from which we can quench a liquid to a glass is constrained by the cooling rate. We were unable to obtain glass samples for $\text{Na}_2\text{Si}_4\text{O}_9$ and $\text{K}_2\text{Si}_4\text{O}_9$ compositions above 12 GPa and 10 GPa, respectively. We did successfully extend the accessible pressure for $\text{Na}_2\text{Si}_2\text{O}_5$ composition to 10 GPa by quenching from a higher temperature than employed during a previous experiment (Xue et al., 1989).

In general, we checked the experimental products optically (400X) to ensure that homogeneous, crystal-free glass samples were obtained. ^{29}Si NMR and Raman spectra are also capable of distinguishing small amounts of crystalline phases from amorphous phases (see below) and indicate that the samples were entirely glassy (see below).

^{29}Si and ^{23}Na MAS NMR spectroscopy

We made MAS NMR measurements with a Varian VXR-400S spectrometer and a MAS probe at a Larmor resonance frequency of 79.459 and 105.800 MHz for ^{29}Si and ^{23}Na respectively. Frequencies were calibrated to ± 0.2 ppm against an external standard of tetramethyl silane (TMS) for ^{29}Si and 1 M aqueous NaCl for ^{23}Na . We used MAS rotors with double O-ring seals to prevent sample hydration, a sample spinning speed of 6–10 kHz, and a 1 μs (about 15° tip angle) radio frequency pulse.

In general, peak areas in ^{29}Si MAS NMR spectra of silicates are quantitatively proportional to site abundances, even in highly disordered, amorphous materials. Exceptions to this occur when delay times between successive pulses are too short to allow complete spin-lattice relaxation combined with unequal relaxation time for different sites, or when the lines are broadened to the point of nonobservability as a result of high levels of paramagnetic impurities, or, conceivably, when there is an extremely wide range of local structural environments. We have studied the former problem in detail and found no changes in relative peak intensities with delay times longer than 1 s in our samples, although absolute intensities did increase up to a delay time of about 120 s. Optimal signal to noise ratios were obtained with the shorter delays. We chose delay times of 1–10 s for the spectra reported in this study. We do not expect paramagnetic line broadening to be significant at the level of Gd_2O_3 added in our samples (0.2 wt%). In order to evaluate the possibility that pressure produced a large range of local structural environments so as to cause loss of signal intensities, we have collected spectra for the $\text{Na}_2\text{Si}_4\text{O}_9$ samples quenched from 8 and 12 GPa with 120 s delays. The signal to noise ratios of these spectra are poor, but are sufficient to allow us to integrate peak areas with a precision of ± 10 –20%. Total areas of these spectra are within error of that of the spectrum for a glass produced on remelting and quenching at 1 atm using the glass quenched from 8 GPa. This confirms our earlier conclusion based on the $\text{Na}_2\text{Si}_2\text{O}_5$ glasses that there is no significant signal intensity loss at high pressures (Xue et al., 1989). The shape of the spectrum of the remelted sample is identical to the glass prepared at 1 atm, indicating that no significant change in composition (<1 mol% in SiO_2 content) occurred during the high pressure experiments.

Raman and infrared spectroscopy

We obtained micro-Raman spectra from 50–200 μm chips of the glass samples using an Instrument S.A. U-1000 double monochromator system and an Innova 90-4 Ar^+ laser for sample excitation. Laser power at the sample was 10–30 mW, and instrument slits were 700 μm (approximately 6 cm^{-1}).

We collected microinfrared reflectance spectra from 25–70 μm relatively flat areas of the glass chips using a Digilab FTS-40 spectrometer equipped with a UMA-300 IR microscope accessory, H_2O -cooled ceramic source, KBr beamsplitter, and broad band (500–6500 cm^{-1}) HgCdTe detector. The mean angle of incidence defined by the 32X Cassegrain objective was about 20° from normal. Considering small departures of the sample surface from planarity and tilted orientations of some samples, the angles of the incident and reflected beams varied between 10° and 35° from normal. Our spectra for the glasses prepared at 1 atm are essentially identical to published spectra obtained with similar angles of incidence (Simon and McMahon, 1953; Sanders et al., 1974). We also observed no orientation effects by obtaining several spectra for each

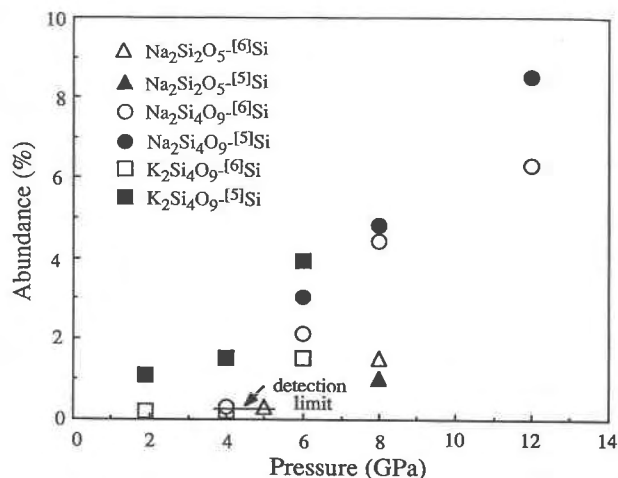


Fig. 1. Abundances of ^{15}Si and ^{16}Si species estimated from ^{29}Si MAS NMR peak areas vs. pressure for alkali silicate glasses quenched from liquids. Data for the 1.9 GPa $\text{K}_2\text{Si}_4\text{O}_9$ glass are from Stebbins and McMillan (1989) (also see Table 1); the rest are from this paper (Table 1).

sample. We used aperture sizes down to $25\ \mu\text{m}$ and observed no interference fringes in any of the spectra in the frequency range down to $500\ \text{cm}^{-1}$. We have also attempted to carry out Kramers-Kronig analyses on these reflectance data to obtain optical constants and the infrared absorption spectrum, but the results were not satisfactory because our reflectivity curves did not extend below $500\ \text{cm}^{-1}$ where additional bands are known to occur. However, previous studies on glasses prepared at 1 atm have shown that the reflection bands are very similar to the absorption spectra, with the reflectance maximum occurring within $20\text{--}30\ \text{cm}^{-1}$ of the absorption peaks (Sweet and White, 1969; Domine and Piriou, 1983). We thus present only the raw reflectance spectra in this paper.

In addition, we observed no absorption in the O-H stretching region confirming that our samples were anhydrous. For some samples, weak features near $1450\ \text{cm}^{-1}$ caused by CO_3^{2-} bending vibrations appear probably resulting from surface reaction with atmospheric CO_2 or residual carbonate in some of the ^{29}Si enriched starting materials.

RESULTS AND SPECTRAL INTERPRETATION

^{29}Si NMR spectroscopy

$\text{Na}_2\text{Si}_2\text{O}_5$ glasses. We have reported ^{29}Si MAS NMR spectra of $\text{Na}_2\text{Si}_2\text{O}_5$ glasses quenched from liquids at 1 atm, 5 GPa, and 8 GPa in an earlier paper (Xue et al., 1989). We observed a peak near $-198\ \text{ppm}$ in the 8 GPa glass and assigned it to ^{16}Si (Xue et al., 1989). Another peak near $-147\ \text{ppm}$, which may be assigned to ^{15}Si as discussed by Stebbins and McMillan (1989), appears simultaneously with ^{16}Si in the 8 GPa $\text{Na}_2\text{Si}_2\text{O}_5$ sample, but was not reported previously because it partially overlaps with a spinning side band (Fig. 1 in Xue et al., 1989). These high-coordination Si species must be part of the

TABLE 1. Abundances of ^{15}Si and ^{16}Si in quenched glasses estimated from peak areas of the ^{29}Si MAS NMR spectra

Samples		^{15}Si	^{16}Si
$\text{Na}_2\text{Si}_4\text{O}_9$	1 atm	<0.05	<0.05
	4 GPa	<0.3	<0.3
	6 GPa	3.0	2.1
	8 GPa	4.8	4.4
	12 GPa	8.5	6.3
$\text{K}_2\text{Si}_4\text{O}_9$	1 atm	<0.05	<0.05
	1.9 GPa*	1.1	0.2
	4 GPa	1.5	0.2
	6 GPa	3.9	1.5
$\text{Na}_2\text{Si}_2\text{O}_5$	1 atm	<0.05	<0.05
	5 GPa	<0.3	<0.3
	8 GPa	≈ 1.0	1.5
SiO_2	6 GPa	<0.3	<0.3

Note: Relative errors are about $\pm 30\%$. Those with upper limits only denote the detection limits.

* Data from Stebbins and McMillan (1989).

glass structure because transmission electron microscopic study has revealed that no crystalline phases are present in this sample (Xue et al., 1989). Neither peak can be detected in the 1 atm and 5 GPa $\text{Na}_2\text{Si}_2\text{O}_5$ samples at a detection limit of about 0.05% and 0.3%, respectively (Xue et al., 1989). These two peaks also appear in the $\text{Na}_2\text{Si}_4\text{O}_9$ and $\text{K}_2\text{Si}_4\text{O}_9$ glasses quenched at high pressures (see below). Since the intensities of both peaks are much higher in the high pressure $\text{Na}_2\text{Si}_4\text{O}_9$ glasses, the assignment of these peaks to ^{15}Si and ^{16}Si species in the glass will be discussed further in conjunction with the spectra of these samples. The abundances of ^{15}Si and ^{16}Si species are reported in Table 1 and Figure 1.

Progressively more pronounced shoulders in the tetrahedral peak attributable to Q^2 and Q^4 species are developed with increasing pressure as shown in the previously published $\text{Na}_2\text{Si}_2\text{O}_5$ spectra (Fig. 3 in Xue et al., 1989). In these samples, the abundances of high coordination Si are probably too low to have a significant influence on the ^{14}Si line shape. Therefore we have quantified these results by fitting the spectra with Gaussian peak shapes and constraining peak areas by mass balance of the following reactions:

$$2Q^3 = Q^4 + Q^2$$

$$2Q^2 = Q^3 + Q^1.$$

The results are shown in Table 2. Although this quantification is nonunique and model dependent, these results support our earlier qualitative conclusion that a major effect of pressure is an increase in the variety of Q species. Our fitting of the 1 atm line shape produces estimated species abundances that are close to those calculated by least squares regression in previous studies and to those derived from static line shapes for this composition (Murdoch et al., 1985; Brandriss and Stebbins, 1988).

$\text{Na}_2\text{Si}_4\text{O}_9$ glasses. The ^{29}Si MAS NMR spectra of the $\text{Na}_2\text{Si}_4\text{O}_9$ glasses quenched at 1 atm and 4, 6, 8, and 12

TABLE 2. Estimated abundances of Q species in Na₂Si₂O₅ quenched glasses

Pressure	Q ¹	Q ²	Q ³	Q ⁴
1 atm		7.9	84.2	7.9
5 GPa		8.4	83.3	8.4
8 GPa	2.8	9.9	71.8	15.5

GPa are shown in Figure 2. As for the Na₂Si₂O₅ composition, there are two major differences in the spectra obtained on a glass prepared at 1 atm vs. those obtained on glasses prepared at high pressure: development of two new peaks near -147 ppm and -198 ppm in the high pressure glasses and change in the shape of the major, ²⁹Si peak.

The two new peaks near -147 ppm and -198 ppm first appear in the glass quenched at 6 GPa and increase in intensity with pressure but are not observable in the 4 GPa glass at a detection limit of about 0.3% (Fig. 2). As we discussed previously (Xue et al., 1989; Stebbins and McMillan, 1989), these features are most reasonably interpreted as resulting from the presence of ¹⁵Si (-147 ppm) and ¹⁶Si (-198 ppm) in an amorphous phase. Only ¹⁶Si is known to produce isotropic chemical shifts in the -180 to -220 ppm range for silicates, having been observed in several crystalline silicate phases (e.g., Kirkpatrick, 1988; Kanzaki et al., 1989; Stebbins and Kanzaki, 1991) and phosphosilicate glasses (Dupree et al., 1987). The assignment of the peak near -147 ppm to ¹⁵Si is consistent with recent theoretical calculations (Tossell and Lazeretti, 1986; Tossell, 1990) and with the systematic change in ²⁷Al chemical shifts from fourfold to fivefold to sixfold coordination (e.g., Kirkpatrick, 1988). ¹⁵Si has not been detected in any crystalline silicate phases, but ¹⁵Al, ¹⁵Ge, and ¹⁵Ti have been observed in a few crystalline phases such as andalusite (Al₂SiO₅) (Taylor, 1929; Burnham and Buerger, 1961), K₂Ge₈O₁₇ (Fay et al., 1973), and K₂Ti₂O₅ (Andersson and Wadsley, 1960), in which the coordination polyhedra are distorted trigonal bipyramids. ¹⁵Al has also been observed in Al₂O₃-SiO₂ and CaO-Al₂O₃-SiO₂ glasses (Risbud et al., 1987; Sato et al., 1989). The occurrence of ¹⁵Si in the quenched glasses, but not in crystals, probably reflects the flexibility of melt structure in accommodating low symmetry units at pressure.

Because NMR chemical shifts are dominated by first and second neighbor effects, further support for these peak assignments can be obtained from a wealth of ²⁹Si NMR spectra on organic liquids (Marsmann, 1981; Cella et al., 1980). For these molecules, the chemical shifts for Si coordinated by six O or C atoms generally fall in the range of -180 to -220 ppm and Si coordinated by five O or C atoms generally fall in the range from -125 to -175 ppm. The only four-coordinated Si species that falls in the latter range is Si linked directly to four other Si atoms which have one Si and three O neighbors with a chemical shift in the -30 to -50 ppm range. Formation of such

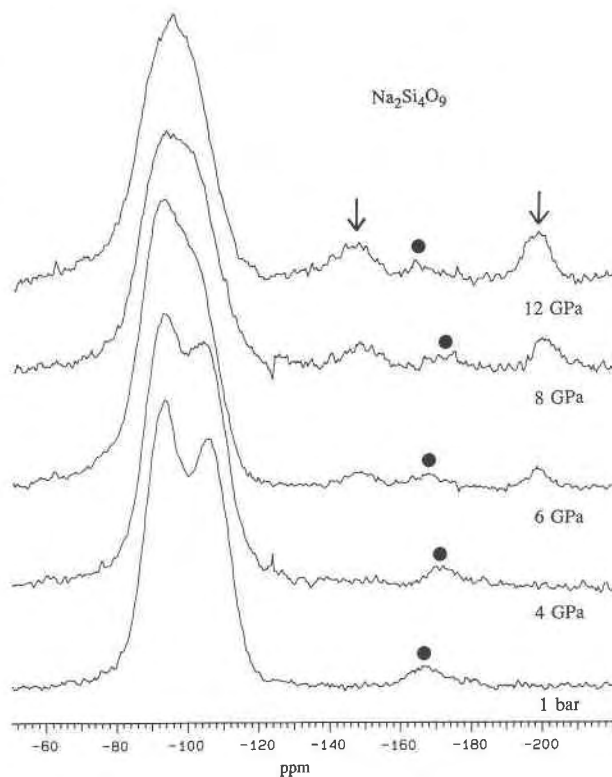


Fig. 2. ²⁹Si MAS NMR spectra of Na₂Si₄O₉ glasses quenched from liquids at 1 atm and 1200 °C, 4 GPa and 1800 °C, 6 GPa and 1900 °C, 8 GPa and 2000 °C, and 12 GPa and 2100 °C. For the 1 atm spectrum, about 100 mg of sample and 10000 signal averages, with 1 s delay time, were used. For the spectra of high-pressure glasses, about 7 mg, and 100 000 signal averages, with the same delay time were used. Solid dots show spinning sidebands, arrows show position of peaks due to ¹⁵Si and ¹⁶Si. Exponential line broadening of 20 Hz (0.13 ppm) was applied for all spectra. Scale in ppm relative to tetramethyl silane (TMS). All spectra were plotted with equal total peak areas.

groups would require very reduced conditions and is unlikely in our samples because there is no evidence for severe sample reduction. The NMR peak expected for the Si-O3Si sites is also absent. It is, of course, conceivable that entirely new types of structures could be formed at high pressures, such as extremely distorted octahedra with two distant and four close O neighbors. Until theoretical work or other observations identify such new species, however, we choose the simpler and better known assignments of ¹⁵Si and ¹⁶Si as most probable.

The observed ¹⁵Si and ¹⁶Si species in our samples are most likely to be part of the glass structure because the full widths at half maximum (FWHM) for both peaks (about 10 ppm) are much broader than typical line widths of about 1 ppm for ¹⁴Si and ¹⁶Si in crystalline alkali and alkaline-earth silicates and silica polymorphs. This contrasting peak width between a crystal and a glass is shown

by the ^{29}Si MAS NMR spectrum for a $\text{Na}_2\text{Si}_4\text{O}_9$ sample quenched from near its liquidus temperature at 12 GPa (Fig. 3). This spectrum is very similar to that for a crystal-free glass quenched at the same pressure (Fig. 2), but has two small superimposed sharp peaks of ^{14}Si and ^{16}Si from a small proportion of a crystalline phase. In the rest of our discussions, only data for completely crystal-free glass samples are used. The abundances of ^{15}Si and ^{16}Si species in the $\text{Na}_2\text{Si}_4\text{O}_9$ glasses quenched from up to 12 GPa are reported in Table 1 and Figure 1.

Changes in the major, ^{14}Si peak for the $\text{Na}_2\text{Si}_4\text{O}_9$ glasses with pressure are also dramatic (Fig. 2). The spectrum for 1 atm $\text{Na}_2\text{Si}_4\text{O}_9$ glass, similar to previous results (e.g., Dupree et al., 1984; Schneider et al., 1987), has a doublet that can be unequivocally assigned to ^{14}Si in Q^3 sites (-92.6 ppm) and in Q^4 sites (-105.5 ppm) by comparison with crystalline materials. In samples from 1 atm to 4 GPa, the Q^4 peak shifts to less negative chemical shift (higher frequency), and appears to broaden slightly as suggested by the decrease in slope at midheight. The Q^3 peak also shifts slightly to the same direction and becomes broader. The largest change in the tetrahedral peak shape occurs between 4 and 6 GPa. The tetrahedral peaks for the glasses quenched above 6 GPa are no longer resolved into two distinct peaks. The 6 GPa spectrum has an asymmetrical tetrahedral peak with the maximum toward the high frequency side. The high frequency side of this peak is shifted slightly to higher frequency and the low frequency side shifted more dramatically in the same direction compared with the spectra obtained from a glass quenched from 4 GPa. In spectra obtained from glasses prepared in the range of 6–12 GPa, this peak becomes progressively more symmetrical. In addition, the intensity in the -65 to -75 ppm region at the high frequency tail of the main peak increases with pressure.

These changes may be associated with at least two factors: formation of high-coordination Si species and changes in the Si-O-Si angles and proportions of Q species. As shown earlier, the 6 to 12 GPa glasses contain a significant amount of ^{15}Si and ^{16}Si . At a concentration level of a few percent for ^{15}Si and ^{16}Si , these species are likely to be isolated from each other and connected with 4–6 ^{14}Si neighbors. In this case, even the 6 GPa sample with its content of 3% ^{15}Si and 2% ^{16}Si would require either over 20% of the ^{14}Si to have one ^{15}Si (or ^{16}Si) neighbor or over 10% of the ^{14}Si with two such neighbors. A change from a ^{14}Si to a ^{15}Si (or ^{16}Si) neighbor should shift a ^{14}Si peak to higher frequency because decreased chemical shielding is associated with longer, more ionic bonds. We have recently confirmed this by ^{29}Si MAS NMR studies on several high pressure crystalline silicates (e.g., wadeite- $\text{K}_2\text{Si}_4\text{O}_9$, garnet- MgSiO_3 , and sodium pyroxene ($\text{NaMg}_{0.5}^{16}\text{Si}_{0.5}^{14}\text{Si}_2\text{O}_6$) (Kanzaki et al., 1989; Stebbins and Kanzaki, 1991). The tetrahedral site in the wadeite- $\text{K}_2\text{Si}_4\text{O}_9$ structure, for example, has two ^{14}Si and two ^{16}Si neighbors, and has an isotropic chemical shift of -96 ppm, deshielded by about 10 ppm from typical Q^4 sites with four

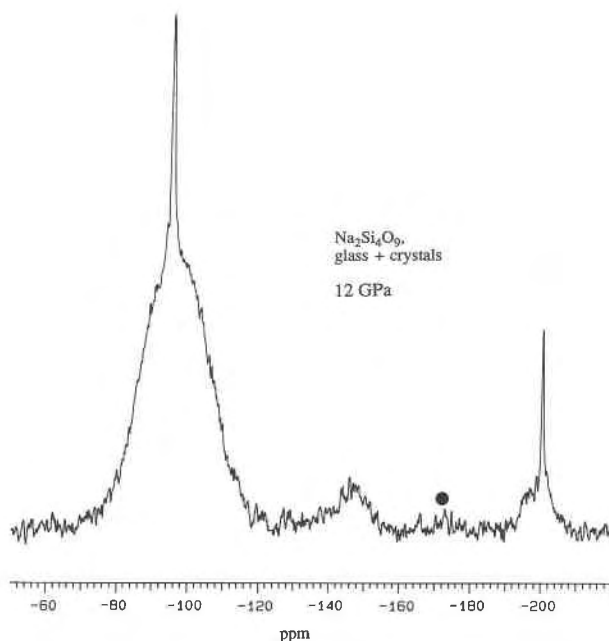


Fig. 3. ^{29}Si MAS NMR spectrum of a $\text{Na}_2\text{Si}_4\text{O}_9$ sample quenched from liquid at 12 GPa and 2000 °C, which is mostly glass with a small amount of crystalline phase. The broad ^{14}Si , ^{15}Si , and ^{16}Si peaks are caused by the glass, whereas the superimposed sharp ^{14}Si and ^{16}Si peaks are caused by crystalline material. Sample size and NMR experimental conditions for this spectra are similar to those for the other spectra of high-pressure glasses in Figure 2. Symbols, scale, and line broadening as in Figure 2.

^{14}Si neighbors (Kanzaki et al., 1989). A ^{14}Si site with three ^{14}Si and one ^{16}Si neighbors might have a chemical shift of about -100 ppm. Similarly, a ^{14}Si site with one or two ^{15}Si neighbors may have chemical shifts between that with one or two ^{16}Si neighbors and that with ^{14}Si neighbors only. The peak shape changes for the 6 to 12 GPa samples can be thus at least partly attributed to the formation of new types of second neighbor connectivities at high pressures, whose peaks overlap with those of the normal Q^3 and Q^4 peaks. In addition, the relative proportions of normal Q^3 and Q^4 species may also change accompanying the formation of high coordination Si and this may contribute to the observed change in ^{14}Si peak shape as well.

On the other hand, changes between the 1 atm and the 4 GPa samples (particularly the shift of peak maxima to higher frequency) may be mainly due to reduction of Si-O-Si angles because there are no detectable high-coordination Si species in these samples. Known correlations (Engelhardt and Radeglia, 1984; Devine et al., 1987; Smith and Blackwell, 1983) suggest a decrease of about 1.1° in the mean Si-O-Si angle for Q^3 , and of about 1.2° for Q^4 from 1 atm to 4 GPa. Pressure-induced reduction of mean Si-O-Si angles may have also occurred in the glasses quenched above 6 GPa, but its effect on the peak posi-

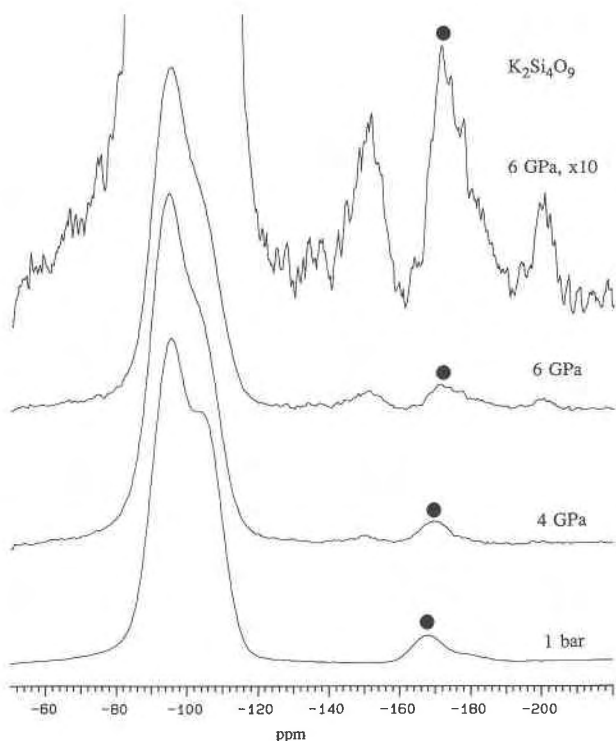


Fig. 4. ^{29}Si MAS NMR spectra of $\text{K}_2\text{Si}_4\text{O}_9$ glasses quenched from liquids at 1 atm and 1200 °C, 4 GPa and 1800 °C, and 6 GPa and 2000 °C. For the spectrum of 1 atm glass, about 90 mg of sample and 10000 signal averages with 10 s delay time were used. For the spectra of 4 and 6 GPa glasses, about 8 mg of sample, and 120 000 and 60000 signal averages respectively with a 1 s delay were used. All spectra are plotted with equal total peak areas except the top one, the vertical scale of which is expanded by 10X. Symbols, horizontal scale, and line broadening as in Figure 2.

tions is not resolvable from that associated with formation of high-coordination Si.

Finally, the increasing intensity in the -65 to -75 ppm region with pressure may be due to an increase in Q^2 species. This suggests that Q-speciation disproportionation reaction as observed in $\text{Na}_2\text{Si}_2\text{O}_5$ glasses may have occurred in the $\text{Na}_2\text{Si}_4\text{O}_9$ samples as well, but the high-silica content of this composition makes the Q^4 peak less sensitive to this effect.

$\text{K}_2\text{Si}_4\text{O}_9$ glasses. The ^{29}Si MAS NMR spectra of the 1 atm, 4 GPa, and 6 GPa $\text{K}_2\text{Si}_4\text{O}_9$ glasses are shown in Figure 4. Peaks of both ^{15}Si and ^{16}Si appear in the spectra for the 4 and 6 GPa samples and increase in intensity with pressure as for the $\text{Na}_2\text{Si}_4\text{O}_9$ glasses (Table 1). The $\text{K}_2\text{Si}_4\text{O}_9$ glasses have more ^{15}Si than the $\text{Na}_2\text{Si}_4\text{O}_9$ glasses at both 4 and 6 GPa (Table 1). These two peaks have also been previously observed at lower intensities in the spectrum of a 1.9 GPa $\text{K}_2\text{Si}_4\text{O}_9$ glass (Stebbins and McMillan, 1989; also see Table 1).

Changes in the tetrahedral peak of the $\text{K}_2\text{Si}_4\text{O}_9$ spectra are again similar to those for the $\text{Na}_2\text{Si}_4\text{O}_9$ composition

(Fig. 4). The spectra of 1 atm glass is again composed of a tetrahedral doublet peak which can be attributed to the presence of Q^3 and Q^4 sites, similar to previously reported $\text{K}_2\text{Si}_4\text{O}_9$ spectra (e.g., Dupree et al., 1986; Grimmer and Muller, 1986; Schneider et al., 1987), but the two peaks are less resolved than in the spectrum of the 1 atm $\text{Na}_2\text{Si}_4\text{O}_9$ glass (Fig. 2). With increasing pressure, the low frequency side of the tetrahedral peak shifts to higher frequency and the doublet becomes less resolved. Again, these changes may be explained by a contribution from reduction of the mean Si-O-Si angle of Q^4 species and perhaps also from development of new ^{14}Si species that share one or more O atoms with a ^{15}Si (or ^{16}Si), especially for the spectrum of 6 GPa glass.

SiO_2 glass. The ^{29}Si static and MAS NMR spectra of a SiO_2 glass quenched from liquid at 6 GPa are shown in Figure 5. The ^{29}Si static spectrum of this sample has a symmetrical peak centered at -109.7 ppm with a FWHM of 28 ppm. The ^{29}Si MAS NMR spectrum has a single symmetrical peak centered at -108.5 ppm with a FWHM of 13 ppm. There is no high-coordination Si species at a detection limit of about 0.3%. Compared with previously reported chemical shift of ^{29}Si MAS NMR spectra of 1 atm SiO_2 glass (e.g., Murdoch et al., 1985: -110.9 ppm; Oestrike et al., 1987: -112.1 ppm), a pressure of 6 GPa shifts the NMR peak to higher frequency by about 2.5–3.5 ppm, corresponding to a reduction of Si-O-Si bond angle of about 4 – 6° (cf. Oestrike et al., 1987), comparable to the extent of change observed in the ^{29}Si MAS NMR spectrum of a SiO_2 glass quenched from 5 GPa and 600 °C (Devine et al., 1987). The density of another SiO_2 glass synthesized under similar condition as for the ^{29}Si enriched sample studied, but with normal Si isotopic composition, is $2.52(1)$ g/cm 3 , which is about 15% higher than glass with normal isotopic composition prepared at 1 atm, again comparable to the extent of densification of the sample by Devine et al. (1987). There is no obvious peak broadening in our sample compared with previous results for 1 atm glasses (Murdoch et al., 1985; Oestrike et al., 1987).

^{23}Na NMR spectroscopy

The ^{23}Na MAS NMR spectra for $\text{Na}_2\text{Si}_2\text{O}_5$ and $\text{Na}_2\text{Si}_4\text{O}_9$ glasses quenched at 1 atm and 8 GPa are shown in Figure 6. For both compositions, the spectra of the high pressure glasses are similar to those of the 1 atm glasses, but have slightly narrower line width (Fig. 6). As is common even in crystalline materials, these line shapes cannot be accurately simulated by a single quadrupolar powder pattern, but require the presence of a range of quadrupolar couplings (Phillips et al., 1988). It is difficult to interpret precisely the pressure effect, but the observed line width decreases could be caused by a slight reduction in the mean quadrupolar coupling constant or by a reduction in the range of values. Either possibility may indicate a more regular or more symmetrical average coordination polyhedron for Na at higher pressures. Such a change probably reflects smaller Na sites at high pressure.

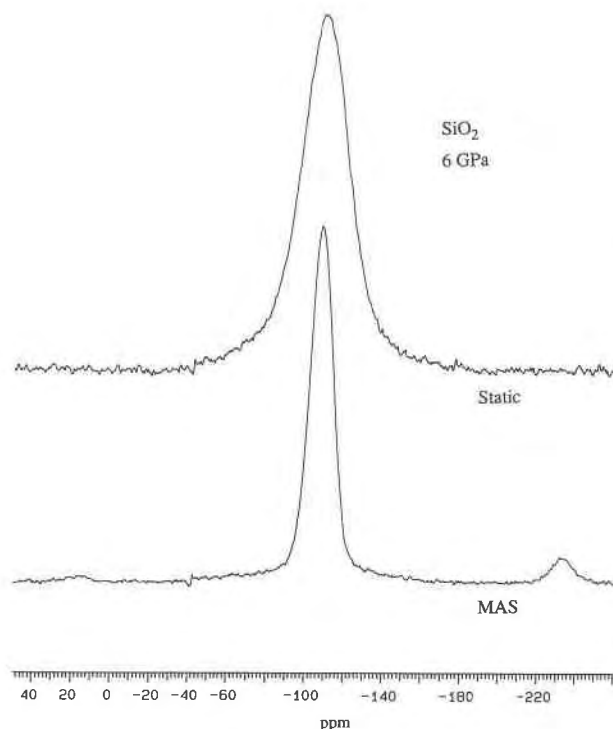


Fig. 5. ^{29}Si static (top) and MAS (bottom) NMR spectra of SiO_2 glass (about 5 mg) quenched from a liquid at 6 GPa and $>2600^\circ\text{C}$. For both spectra, about 50000 signal averages with 1 s delay time were used. Exponential line broadening of 50 Hz (0.32 ppm) was applied for both spectra.

Raman and infrared spectroscopy

$\text{Na}_2\text{Si}_2\text{O}_5$ glasses. Raman spectra for the 1 atm, 5 GPa, and 8 GPa $\text{Na}_2\text{Si}_2\text{O}_5$ glasses with 95% ^{29}Si enriched compositions used in the NMR study (Xue et al., 1989; also this paper) and a 10 GPa glass with normal Si isotopic composition are shown in Figure 7. The Raman spectrum of the 1 atm $\text{Na}_2\text{Si}_2\text{O}_5$ glass is identical to those reported previously (Brawer and White, 1975; Furukawa et al., 1981; Matson et al., 1983) except for small frequency shifts resulting from the ^{29}Si isotopic substitution. The strong high frequency peak at 1090 cm^{-1} can be attributed to the symmetric Si-O stretching of Q^3 species within the glass, and the weak peak at 940 cm^{-1} is caused by Si-O stretching of Q^2 species. The 772 cm^{-1} band may correspond to motions of Si against its tetrahedral oxygen cage. Raman bands in the $500\text{--}600\text{ cm}^{-1}$ region are associated with bending vibrations of the Si-O-Si linkage, and the frequencies of these bands depend on the Si-O-Si angle and degree of polymerization of the silicate units (McMillan, 1984). The major peak at 562 cm^{-1} in the spectrum of the 1 atm $\text{Na}_2\text{Si}_2\text{O}_5$ glass is most likely caused by Si-O-Si bending vibration of linkages associated with the predominant Q^3 species. This peak is asymmetric with an unresolved component near 600 cm^{-1} on its high frequency side attributable to a population with narrower Si-O-Si angles in the glass. This shoulder has often been assigned to Si-O-Si vibration of linkages associated with

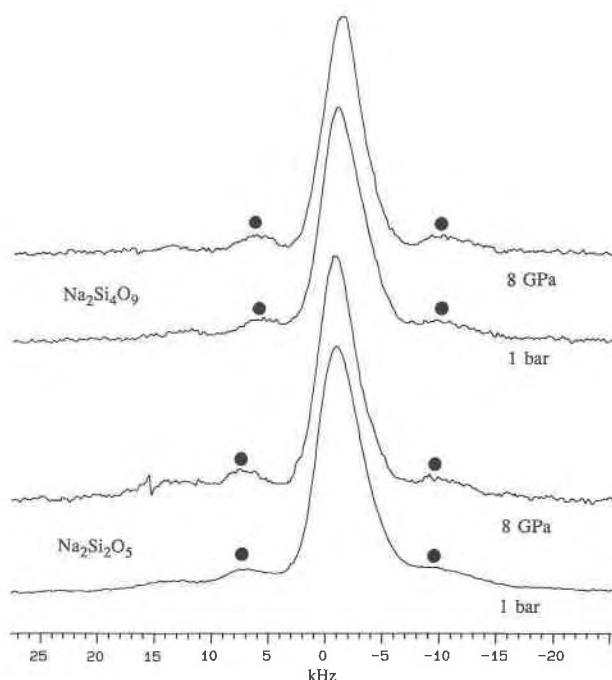


Fig. 6. ^{23}Na MAS NMR spectra for the $\text{Na}_2\text{Si}_4\text{O}_9$ glasses described in Figure 2 (top) and the $\text{Na}_2\text{Si}_2\text{O}_5$ glasses studied in Xue et al. (1989) (bottom). About 10000 signal averages, 1 s delay, and 200 Hz line broadening were used in each spectrum. Scale in kHz relative to 1 M aqueous NaCl.

the Q^2 species, but Matson et al. (1983) suggested that this feature results from the presence of three-membered siloxane rings containing both Q^4 and Q^3 species in the glass (also see Dickinson et al., 1990). There is also a weak maximum near 430 cm^{-1} probably indicating the presence of Q^4 species as detected by the ^{29}Si NMR experiments.

With increasing pressure the intensity of the 940 cm^{-1} peak relative to the 1090 cm^{-1} peak increases (Table 3), indicating an increase in the proportion of Q^2 species as consistent with observations from the NMR spectra. The 772 cm^{-1} band shows little change in either intensity or position. The low frequency 562 cm^{-1} peak at 1 atm shifts to a slightly higher frequency with pressure and becomes more symmetric because of the growth of its high frequency shoulder. This peak shift suggests a slight reduction of Si-O-Si angle within the Q^3 units with increasing pressure. The growth of its high frequency shoulder could be interpreted as due to increased proportion of either Q^2 species or three-membered siloxane rings. The 430 cm^{-1} feature in the 1 atm glass also moves to higher frequency with increasing pressure, indicated by the angle with which it meets the main $560\text{--}580\text{ cm}^{-1}$ peak. This suggests a narrower mean Si-O-Si angle within the Q^4 units of the glass. Reduction in the mean Si-O-Si angle for Q^4 species has also been observed in previous Raman studies on pressure-densified SiO_2 glasses (McMillan et al., 1984; Hemley et al., 1986).

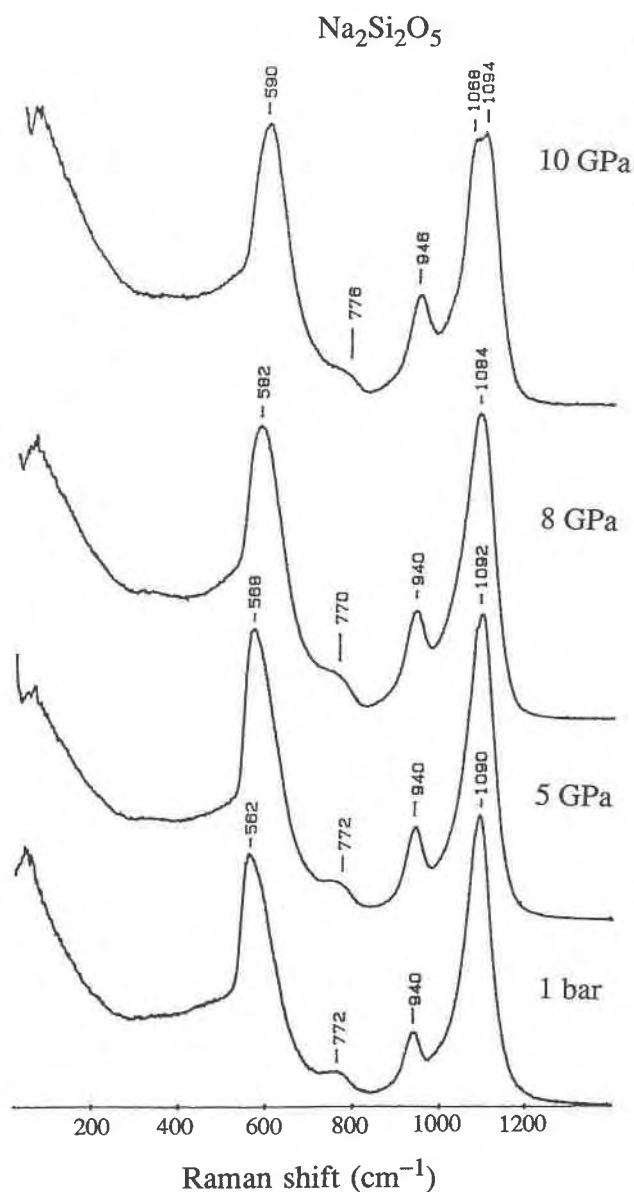


Fig. 7. Unpolarized Raman spectra for $\text{Na}_2\text{Si}_2\text{O}_5$ glasses quenched from liquids. The 1 atm, 5 GPa, and 8 GPa samples are those studied by Xue et al. (1989) and have 95% ^{29}Si enriched compositions. The 10 GPa sample was quenched from 1800 °C and has normal Si isotopic composition (92% ^{28}Si).

There is also a significant change in the 1090 cm^{-1} band with increasing pressure. There is a break near the peak maximum for the spectrum of the 5 GPa glass, suggesting the appearance of a second unresolved peak at lower wavenumber. This unresolved peak is no longer visible in the spectrum of 8 GPa glass, but the FWHM of the main peak is greater than for the spectrum of 5 GPa glass (Table 3), suggesting continued growth of this second, unresolved peak. In the spectrum of 10 GPa glass, this high frequency peak clearly shows two maxima at 1068

TABLE 3. Features of the Raman spectra of $\text{Na}_2\text{Si}_2\text{O}_5$ glasses

Pressure	Si isotopic composition	a	b
1 atm	95% ^{29}Si	0.13 ± 0.1	$75 \pm 2 \text{ cm}^{-1}$
5 GPa	95% ^{29}Si	0.18 ± 0.1	$80 \pm 2 \text{ cm}^{-1}$
8 GPa	95% ^{29}Si	0.18 ± 0.1	$88 \pm 2 \text{ cm}^{-1}$
10 GPa	92% ^{28}Si	0.22 ± 0.1	

Note: a = relative height of 940 cm^{-1} vs. 1090 cm^{-1} peaks; b = FWHM for the 1090 cm^{-1} band.

and 1094 cm^{-1} , which possibly correspond to the two unresolved peaks in the spectra of glasses prepared at lower pressures but are better resolved because of the different isotopic composition of the 10 GPa glass. The presence of these two peaks may indicate that two types of Q^3 species are present in the high pressure samples which could be partly responsible for the broadening in the ^{29}Si MAS NMR spectra.

The infrared reflectance spectra of these glasses are shown in Figure 8. The spectrum of the 1 atm glass shows two strong maxima at 1060 and 913 cm^{-1} and a weak band at 740 cm^{-1} . The high frequency peaks are caused by asymmetric Si-O stretching vibrations, but cannot be readily assigned. The valence force field calculations of Dowty (1987) suggest that these two high frequency bands have contributions from relative Si-O displacements involving both bridging and nonbridging O atoms. The weak band near 740 cm^{-1} is generally assigned to a vibration of Si against its oxygen cage (McMillan, 1984; Dowty, 1987).

With increasing pressure, both the 1060 and 913 cm^{-1} peaks of the spectrum of 1 atm glass show a general frequency increase. The 740 cm^{-1} band of the spectrum shows a slight frequency decrease between 5 GPa and 8 GPa. The spectrum of the 10 GPa sample is quite different from those of the lower pressure glasses in both peak positions and intensities, but these changes may be partly due to the $^{28}\text{Si}/^{29}\text{Si}$ isotopic substitution. There are no obvious additional bands in these spectra that might indicate the presence of high-coordination Si sites.

In brief, neither the Raman nor the infrared spectra of $\text{Na}_2\text{Si}_2\text{O}_5$ glasses show additional peaks that might be associated with high-coordination Si sites, possibly because the percentage of these species are small (as shown by the ^{29}Si NMR data). Changes in the Raman spectra can be interpreted as being caused by a small reduction of the mean Si-O-Si angles within Q^3 and Q^4 units and growth of Q^2 species, consistent with a disproportionation reaction with increasing pressure.

$\text{Na}_2\text{Si}_4\text{O}_9$ glasses. Raman spectra for the $\text{Na}_2\text{Si}_4\text{O}_9$ glasses quenched at 1 atm and 4, 6, 8, and 12 GPa are shown in Figure 9. These samples are the same 95% ^{29}Si enriched glasses that were used for the NMR study. Again, the spectrum for the 1 atm glass is identical to those obtained in previous studies (Brawer and White, 1975; Furukawa et al., 1981; Matson et al., 1983). As for the 1 atm $\text{Na}_2\text{Si}_2\text{O}_5$ glass, the strong high frequency peak at 1090

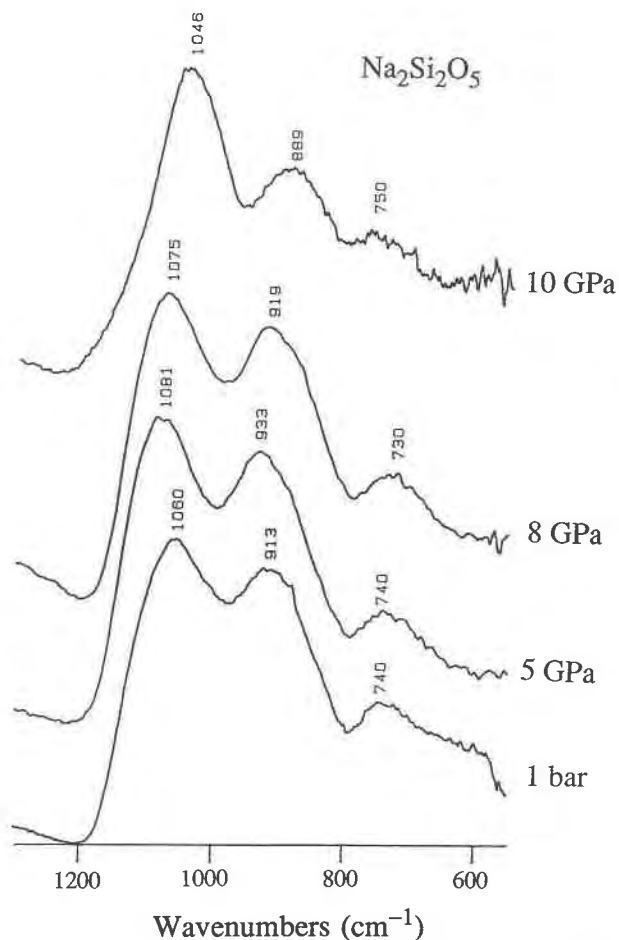


Fig. 8. Microinfrared specular reflectance spectra of $\text{Na}_2\text{Si}_2\text{O}_5$ glasses described in Figure 7.

cm^{-1} is caused by symmetric Si-O stretching vibration of Q^3 species, and the weak peak near 940 cm^{-1} can be assigned to a small proportion of Q^2 species. The 776 cm^{-1} band may correspond to motions of Si against its oxygen cage. The sharp low frequency peak at 522 cm^{-1} may again be attributed to the Si-O-Si bending vibration associated with Q^3 species, and the 598 cm^{-1} maximum on its high frequency shoulder is caused by a population of Si-O-Si linkages in the glass with narrower Si-O-Si angles possibly associated with Q^2 species or three-membered siloxane rings containing both Q^4 and Q^3 species (Matson et al., 1983; Dickinson et al., 1990). The band near 450 cm^{-1} forming a low frequency shoulder on the 522 cm^{-1} peak may be assigned to Si-O-Si bending vibrations of Q^4 species in the glass. The presence of Q^4 species may also be responsible for the maximum near 1156 cm^{-1} on the high frequency shoulder of the 1090 cm^{-1} band (Furukawa et al., 1981; Matson et al., 1983; McMillan, 1984).

There are only very subtle differences between the spectra of the 1 atm and the 4 GPa glasses. The 522 cm^{-1} peak shows a slight shift to higher frequency (526 cm^{-1}), consistent with a slight decrease in Si-O-Si angle within

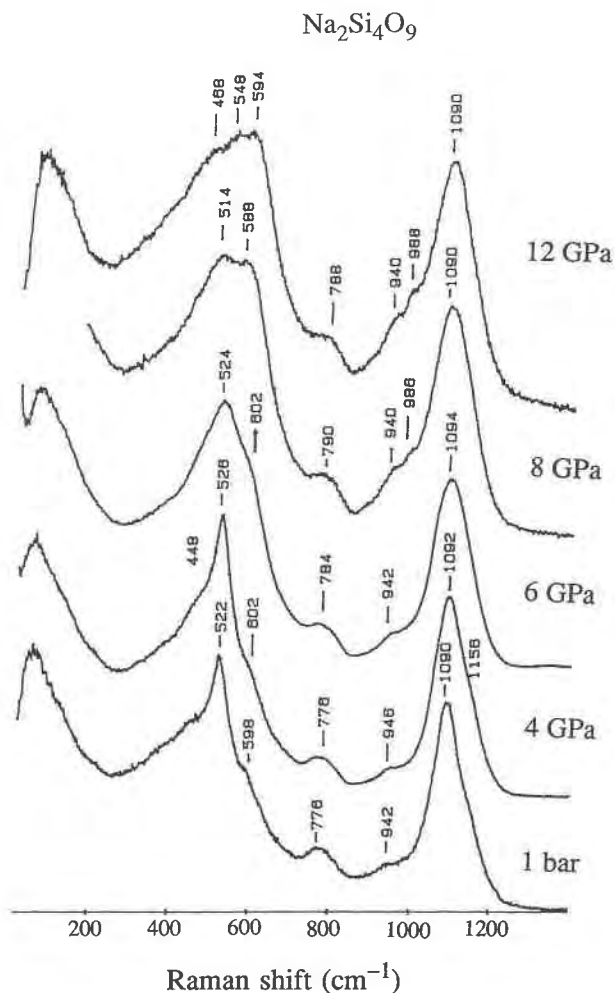


Fig. 9. Unpolarized Raman spectra for $\text{Na}_2\text{Si}_4\text{O}_9$ glasses with 95% ^{29}Si enriched compositions described in Figure 2.

the Q^3 units. The low frequency shoulder on this peak associated with Q^4 species also shifts to higher frequency, suggesting a decrease in mean Si-O-Si angle within the Q^4 units. These changes in bond angle are consistent with the ^{29}Si NMR results for this composition and are also similar to those observed in the Raman spectra of $\text{Na}_2\text{Si}_2\text{O}_5$ glasses. There is no change in the 776 cm^{-1} band.

Above 4 GPa, there are marked changes in the Raman spectra. The intensity of the band near 600 cm^{-1} increases dramatically with increasing pressure and becomes the dominant low frequency band for the 12 GPa sample. Concurrently, there is a large intensity increase in the $250\text{--}550 \text{ cm}^{-1}$ region. An increase in the peak intensity also occurs in the region of the band near 940 cm^{-1} , and an extra weak band near 990 cm^{-1} develops in the 8 and 12 GPa glasses. In addition, the 1156 cm^{-1} maximum on the high frequency shoulder of the 1090 cm^{-1} band is no longer resolved from the main peak for the 6–12 GPa samples. The band near 780 cm^{-1} shifts slightly to higher frequency.

These spectral changes bear a general resemblance to those of the 1 atm $R_2Si_4O_9$ glass series when R is changed from Cs, to Rb, to K, to Na, to Li, during which a disproportionation reaction involving Q^3 is known to occur (Matson et al., 1983). Therefore a simple first-order interpretation for the Raman spectra of these high pressure glasses would be that a pressure-induced disproportionation reaction has occurred as was the case in the $Na_2Si_2O_7$ glasses. The extra intensity in the 900–1000 cm^{-1} region may be caused by increased Q^2 abundances, and the increased intensity in the 250–550 cm^{-1} region could be due to increased Q^4 abundances. The increased intensity in the band near 600 cm^{-1} may be attributed to formation of either additional Q^2 species or three-membered siloxane rings in the high pressure glass samples.

However, the ^{29}Si NMR results suggest that the above interpretation is too simple. NMR data show that a significant amount of high-coordination Si species is present in the 6–12 GPa glasses. Some of the observed changes in the Raman spectra could thus be caused by vibrations of these high-coordination Si species. Furthermore, as discussed in the NMR section, the presence of these species affect the proportions of normal Q species and also require some of the tetrahedral Si sites to share corners with high-coordination Si species. Therefore, even if characteristic vibrations of the high-coordination Si species are not directly observable in the Raman spectra, they must affect the relative intensities of peaks caused by normal Q species and also alter the vibrational modes associated with those tetrahedral Si sites that share O atoms with high-coordination Si species.

Insight about vibrational modes involving both ^{44}Si and ^{66}Si may be derived from Raman spectra of crystalline phases containing these species. In particular, a strong Raman mode at 600 cm^{-1} has been identified in garnet- $MgSiO_3$ as a bending vibration within the $^{44}Si-O-^{66}Si$ linkages (McMillan et al., 1989). Strong peaks in the 500–650 cm^{-1} region have also been observed in wadeite- $K_2Si_4O_9$ (Geisinger et al., 1987) and can be assigned to either the $^{44}Si-O-^{44}Si$ linkage within the three-membered ring of SiO_4 tetrahedra or the $^{44}Si-O-^{66}Si$ linkage. The growth of the 600 cm^{-1} band in the high pressure $Na_2Si_4O_9$ glasses could thus be caused by growth of one or more of the following structural units: (1) Q^2 species; (2) three-membered rings; or (3) $^{44}Si-O-^{66}Si$ (and $^{44}Si-O-^{66}Si?$) linkages with increasing pressure.

In addition, high pressure crystalline phases containing only ^{66}Si have Raman modes in the 900–1000 cm^{-1} and 400–600 cm^{-1} regions. The former can be assigned to $^{66}Si-O$ stretching vibrations and the latter may be associated with bending and deformation vibrations of the highly coordinated silicate groups (McMillan and Ross, 1987; Williams et al., 1987; Hemley et al., 1986). It is thus possible that the new weak peak near 990 cm^{-1} that appears in the 8 and 12 GPa spectra and the increased intensity and broadening in the low frequency region (250–550 cm^{-1}) of the 6–12 GPa spectra are also associated with the presence of high-coordination Si groups.

Infrared reflectance spectra for these glasses are shown in Figure 10. The 1 atm glass has a reflectivity maximum near 1083 cm^{-1} with a high frequency shoulder near 1150 cm^{-1} and a low frequency shoulder at 975 cm^{-1} . There is also a weak band at 762 cm^{-1} . With increasing pressure, the low frequency shoulder increases in relative intensity to become the dominant peak at 979 cm^{-1} , while the high frequency shoulder is no longer apparent in the spectrum of the 12 GPa glass. The 762 cm^{-1} band in the spectrum of the 1 atm glass shifts slightly toward lower frequency at high pressures.

Although the assignments of the infrared peaks are not well understood, they may provide some constraints on the structural interpretation by comparison with the compositional trends in the infrared spectra of 1 atm glass. As discussed earlier, we cannot rule out the interpretation of pressure-induced disproportionation of Q^3 species into Q^4 and Q^2 as the main structural change based solely on the observation of Raman spectra. Disproportionation of Q^3 species in $R_2Si_4O_9$ glasses at 1 atm is known to result in increased intensities in both the 975 cm^{-1} shoulder and the 1100–1150 cm^{-1} region as R changes from K, to Na, then to Li (Crozier and Douglas, 1965). The intensity in the 975 cm^{-1} region indeed increases in the high pressure glasses, but there is no corresponding large intensity increase in the 1100–1150 cm^{-1} region. Therefore, such a simple interpretation derived from the Raman spectra cannot fully account for changes in the infrared spectra. In the discussion of the Raman spectra, we inferred that the weak band near 988 cm^{-1} observed for the 8 and 12 GPa samples may be due to $^{66}Si-O$ stretching vibrations. It is also possible that this weak Raman band corresponds to the strong infrared mode near 979 cm^{-1} that increases in intensity with increasing pressure. This could either correspond to an Si-O stretching vibration of the high coordination Si species (^{66}Si or ^{63}Si) as discussed above, or an asymmetric stretching vibration in the $^{44}Si-O-^{66}Si$ (or $^{44}Si-O-^{63}Si$) linkages. Strong infrared absorption is commonly observed in the spectra of crystalline silicates containing only ^{66}Si or structures with mixed $^{44}Si-O-^{66}Si$ linkages (Williams et al., 1987; McMillan et al., 1989).

In summary, the Raman and infrared spectra of $Na_2Si_4O_9$ glasses are consistent with the occurrence of high-coordination Si species in the high pressure samples, although the peak assignments to the vibrational modes involving these species are not unique. Reduction of Si-O-Si angle within Q^3 and Q^4 units with pressure are again suggested by the Raman spectra.

$K_2Si_4O_9$ glasses. Raman spectra, shown in Figure 11, were obtained for $K_2Si_4O_9$ glasses quenched at 1 atm, and 1.9, 4, 5, 6, and 8 GPa. The 1.9 GPa and 4 GPa samples were the same ^{29}Si enriched glasses used for the ^{29}Si NMR (Stebbins and McMillan, 1989; this paper), the rest were those with normal Si isotopic composition. The spectrum of 1 atm glass is again identical to those previously reported (Brawer and White, 1975; Matson et al., 1983) and similar to that of the 1 atm $Na_2Si_4O_9$ glass, but better resolved, especially in the low frequency region. There is

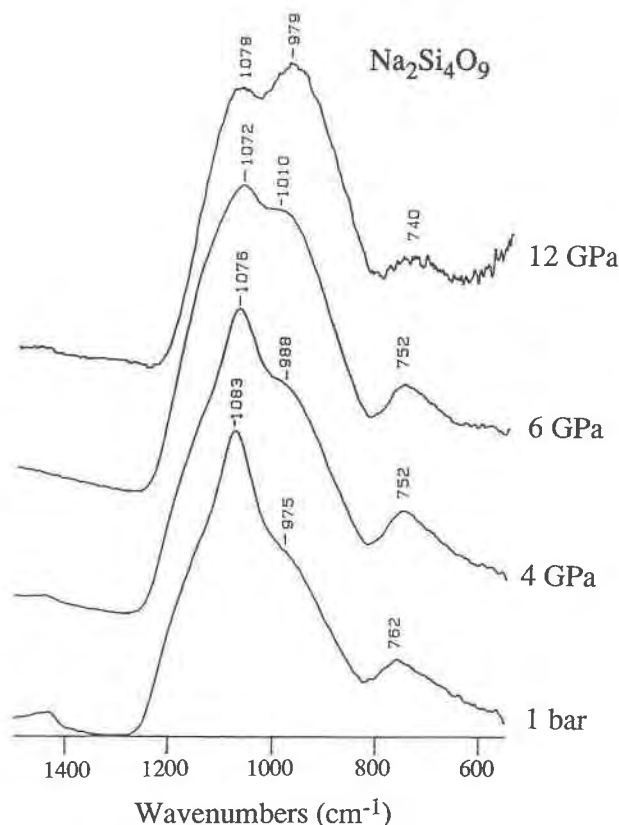


Fig. 10. Microinfrared specular reflectance spectra of $\text{Na}_2\text{Si}_4\text{O}_9$ glasses described in Figures 2 and 9.

less intensity in the $400\text{--}500\text{ cm}^{-1}$ region than in the spectra for $\text{Na}_2\text{Si}_4\text{O}_9$ glasses probably because fewer Q^4 species are present (Matson et al., 1983). The 592 cm^{-1} peak is well resolved from the 520 cm^{-1} band. As described above, these peaks can be attributed to bending vibrations of Si-O-Si linkages. Again the 592 cm^{-1} band is caused by Si-O-Si linkages within the glass with smaller Si-O-Si angle than those associated with the predominant Q^3 species. These narrower Si-O-Si angles might be associated with either the presence of Q^2 species indicated by the weak shoulder in the $900\text{--}1000\text{ cm}^{-1}$ region, or with three-membered siloxane rings in the glass (Matson et al., 1983; Dickinson et al., 1990). The band at 774 cm^{-1} may again be due to Si motion against its oxygen cage. In the high frequency region, there is a well-developed shoulder at 1158 cm^{-1} on the 1102 cm^{-1} band. This shoulder is also present in the 1 atm $\text{Na}_2\text{Si}_4\text{O}_9$ glass and may be associated with the presence of Q^4 species for that glass. Such may not be the case for the $\text{K}_2\text{Si}_4\text{O}_9$ glass because there is much less intensity in the $400\text{--}500\text{ cm}^{-1}$ region that can be attributed to Q^4 species. The 1158 cm^{-1} shoulder is, however, more pronounced. It is likely that this 1158 cm^{-1} feature is due to a second type of Q^3 group in the 1 atm glass, perhaps associated with the presence of small siloxane rings within the glass structure (Matson et al., 1983; Dickinson et al., 1990).

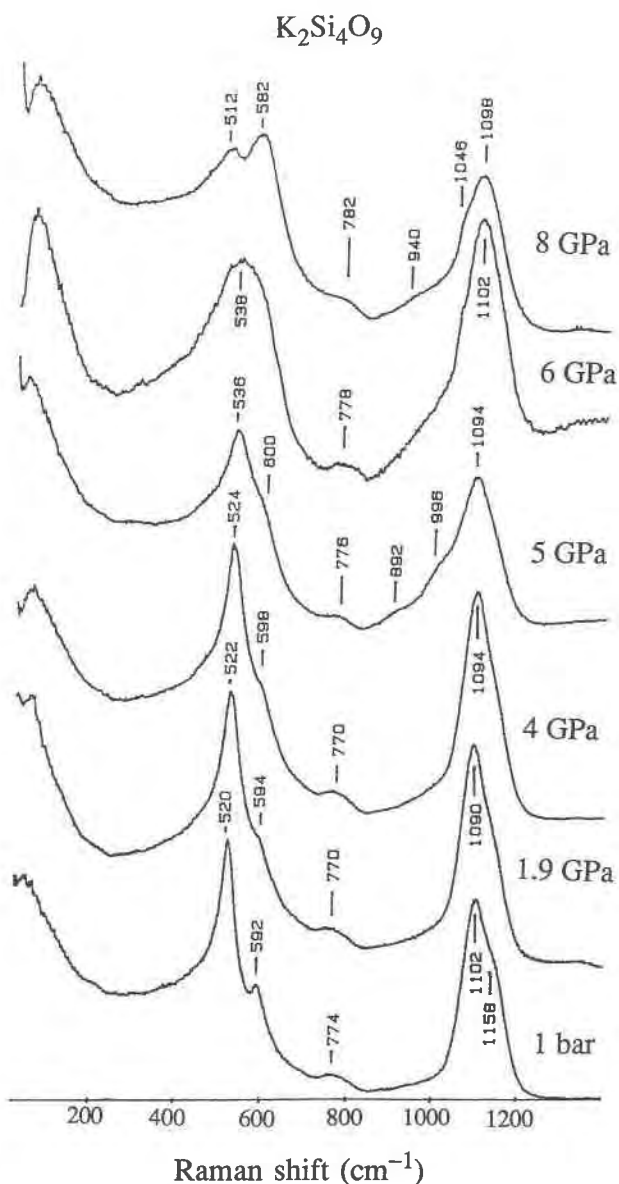


Fig. 11. Unpolarized Raman spectra for $\text{K}_2\text{Si}_4\text{O}_9$ glasses quenched from liquids. The 1.9 GPa and 4 GPa samples contain 95% ^{29}Si . The 1.9 GPa sample was described in Stebbins and McMillan (1989), and the 4 GPa sample is described in Figure 4. The 1 atm and 5, 6, and 8 GPa samples have normal Si isotopic abundance. The 5 GPa sample was quenched from $1700\text{ }^\circ\text{C}$, the 6 GPa sample quenched from $1900\text{ }^\circ\text{C}$, and the 8 GPa sample quenched from $2000\text{ }^\circ\text{C}$.

Raman spectral changes with increasing pressure for this composition are generally similar to those observed for the $\text{Na}_2\text{Si}_4\text{O}_9$ glasses. Only minor changes occur in the spectra of glasses prepared below 5 GPa. The 520 cm^{-1} band moves to higher frequency indicating narrowing of the Si-O-Si angles associated with the major Q^3 species, and there is development of a shoulder near 440 cm^{-1} . Both the 1158 cm^{-1} shoulder and the 592 cm^{-1} band appear to decrease slightly in relative intensity, and weak

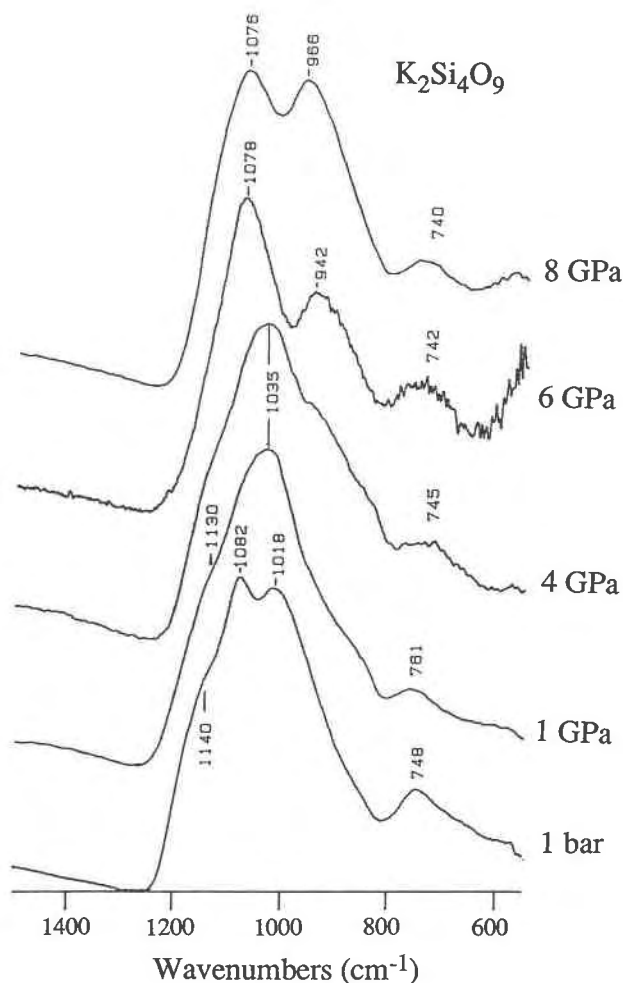


Fig. 12. Microinfrared specular reflectance spectra of $K_2Si_4O_9$ glasses quenched from liquids. The 1 GPa sample was described in Dickinson et al. (1990) and has normal Si isotopic composition. The rest are described in Figure 11.

bands develop near 942 and 986 cm^{-1} . The 942 cm^{-1} feature first appears at approximately 1.5 GPa (Dickinson et al., 1990).

Between 5 GPa and 8 GPa, there is a continued increase in the intensity of the bands in the 900–1000 cm^{-1} region. The 520 cm^{-1} peak of the 1 atm glass has increased in frequency to 536 cm^{-1} by 5 GPa. This forms the central part of the low frequency maximum for the 6 GPa glass, but is no longer seen in the spectrum of 8 GPa glass. A band near 580 cm^{-1} grows to become the dominant low frequency peak for the 8 GPa glass. A new low frequency band near 510 cm^{-1} is first observed as a shoulder in the spectra of 5 and 6 GPa glasses, and is resolved as a band in the 8 GPa spectrum. The band near 770 cm^{-1} shifts slightly to higher frequency. In the high frequency region, a new band near 892 cm^{-1} first develops in the spectrum of 5 GPa glass, and a shoulder near 1046 cm^{-1} on the 1098 cm^{-1} band and a weak feature near 1330 cm^{-1} are observed in the spectra of 6 and 8 GPa glasses.

The interpretation of these spectral changes suffers from ambiguities similar to that for the $Na_2Si_4O_9$ spectra. Again the $K_2Si_4O_9$ glass spectra could be qualitatively interpreted in terms of a pressure-induced disproportionation reaction of Q^3 species with pressure. However, from the ^{29}Si NMR data, it is known that 1.7% of the Si atoms are in fivefold or sixfold coordination in the 4 GPa glass sample. As discussed for the Raman spectra of $Na_2Si_4O_9$ glasses, it would be tempting to assign one or both of the features near 940 cm^{-1} and 990 cm^{-1} either to vibrations of SiO_5 or SiO_6 groups in the glass, or to Si-O stretching vibrations of SiO_4 groups connected to ^{15}Si or ^{16}Si . Likewise, the new bands in the 500–600 cm^{-1} region could be caused by $^{14}Si-O-^{16}Si$ (or $^{14}Si-O-^{15}Si$) linkages, or to $^{14}Si-O-^{14}Si$ linkages forced into unusual geometries by the presence of high-coordination Si species. However, as shown above, new bands are also observed at 892 and 1046 cm^{-1} for the 5–8 GPa $K_2Si_4O_9$ glasses, but we cannot yet assign them.

The infrared reflectance spectra of the glasses described above as well as a 1 GPa glass with normal Si isotopic composition described in Dickinson et al. (1990) are shown in Figure 12. The spectrum of 1 atm glass shows two well-resolved reflectance peaks at 1018 and 1082 cm^{-1} and a shoulder at 1140 cm^{-1} . Between 1 atm and 1 GPa, the 1018 and 1082 cm^{-1} bands coalesce to give a band with principle maximum near 1035 cm^{-1} and the shoulder moves to about 1130 cm^{-1} . Because these bands are in part due to asymmetrical vibrations of Si-O-Si linkages in the glass, this can be correlated with the loss of resolution in the 500–600 cm^{-1} region of the Raman spectrum. At 6 and 8 GPa, the high frequency band increases in frequency to about 1078 cm^{-1} , and a new band develops in the 940–970 cm^{-1} region. As for the discussion of the infrared spectra for the high pressure $Na_2Si_4O_9$ glasses, the growth of the band in the 940–970 cm^{-1} region may be correlated with the increase in the proportion of ^{15}Si and ^{16}Si species in the glass as determined by ^{29}Si NMR. The infrared spectrum of the 8 GPa $K_2Si_4O_9$ glass is similar to and intermediate between the spectra of the 12 GPa and 6 GPa $Na_2Si_4O_9$ glasses in terms of relative band intensities. If our interpretation is correct, it seems likely that the 8 GPa $K_2Si_4O_9$ glass could contain 10–15% of high-coordination Si.

DISCUSSION

Relations between the structure of quenched glasses and liquids

A fundamental uncertainty with spectra obtained on glasses quenched from liquids at high pressures is the extent to which they reflect the structure of the liquids above their liquidus at high pressures. Possible structural changes may be involved in two steps of the procedure: (1) liquid structural changes during temperature quench at high pressure; (2) structural adjustment of the quenched glasses during decompression at room temperature. We will discuss the latter first.

Direct studies of structural relaxation during decompression for glasses quenched from liquids at high pressures have not been attempted. But the problem of structural relaxation for glasses densified at room temperature have been studied. It has been recognized that the structure of silicate glasses densified at room temperature generally relaxes to some extent upon decompression (Hemley et al., 1986; Williams and Jeanloz, 1988; Wolf et al., 1990). Raman studies on SiO_2 and $\text{Na}_2\text{Si}_2\text{O}_7$ glasses at room temperature and pressures up to 50 GPa showed significant changes that were partially preserved during decompression, but certain features of the spectra relaxed on decompression including an apparent increase in the abundances in Q^2 and Q^4 species at the expense of Q^3 species (Hemley et al., 1986; Wolf et al., 1990). However, these results do not necessarily imply that similar relaxation should occur for glasses quenched from liquids at high pressures. The most significant difference between glasses densified at room temperature and those quenched from a liquid at high temperature is that the former did not reach equilibrium at high pressures. McMillan et al. (1984) collected Raman spectra on SiO_2 glass densified at 530 °C and 3.95 GPa and noticed that more structural changes were achieved and preserved than SiO_2 glasses densified at similar pressure, but room temperature. It is thus possible that the extent of structural relaxation during decompression for glasses quenched from liquids might be smaller than for glasses densified at room temperature.

At least at 1 atm, it is generally assumed that the structure of a quenched glass represents that of the liquid at its glass transition temperature (T_g) (e.g., Gibbs and DiMarzio, 1958). This assumption may be extended to high pressure and our samples may, to a first approximation, record the structure of the melts at T_g assuming that structural relaxation during decompression is insignificant. T_g is both cooling rate and pressure dependent. The differences in cooling rate for our samples quenched at different pressures are small and may therefore have a negligible effect on T_g (Brandriss and Stebbins, 1988; also see Xue et al., 1989). But pressure-induced change in T_g may be significant, and therefore the structural changes observed in the quenched glasses may reflect those in the melt structure as a result of variations in both temperature (T_g) and pressure. Direct experimental measurements of T_g at high pressures are scarce, however. At 1 atm, the glass transition as determined by changes in heat capacity or thermal expansion is well correlated with a viscosity of 10^{12} Pa·s for a wide variety of liquids (e.g., Litovitz, 1960). A relation between the effects of pressure on viscosity and on T_g may therefore be expected for silicates. Measurement of T_g up to 0.7 GPa on albite, diopside, and sodium trisilicate glasses are in support of this suggestion (Rosenhauer et al., 1979). The viscosities of melts in the composition range of $\text{Na}_2\text{Si}_2\text{O}_7$ - SiO_2 decrease with increasing pressure at least up to 3 GPa (Scarfe et al., 1979). Viscosity data beyond 3 GPa are not available, but have been predicted to decrease with pressure

based on molecular dynamic simulations (Angell et al., 1982, 1983). It is thus possible that T_g for the presently studied systems decrease with pressure.

Increasing temperature (T_g) is known to enhance Q speciation disproportionation for alkali silicate melts (Brandriss and Stebbins, 1988). A decrease of T_g would thus produce an effect opposite to our observations. Therefore the extent of Q speciation disproportionation observed for $\text{Na}_2\text{Si}_2\text{O}_7$ glasses probably underestimates that of the isothermal pressure effect on the liquid structure near T_g .

The distribution of ^{44}Si , ^{47}Si , ^{49}Si species may also be affected by a variation in temperature (T_g), but this effect is poorly constrained at present. A NMR study of Al_2O_3 - SiO_2 and $\text{CaO-Al}_2\text{O}_3$ - SiO_2 glasses quenched at 1 atm suggests that the proportions of Al in different coordination states are dependent on quench rate (T_g) (Sato et al., 1989). Another NMR study of $\text{Na}_2\text{O} \cdot 2\text{SiO}_2 \cdot 4\text{P}_2\text{O}_5$ glasses suggests that the proportion of ^{16}Si is lower in these glasses when quenched at lower rate (lower T_g) (Dupree et al., 1989). On the other hand, the ^{11}B NMR spectra of calcium aluminoborosilicate glasses quenched at 1 atm show a higher average B coordination (^{11}B is favored over ^{13}B) at lower quench rate (lower T_g) (Gupta et al., 1985). An X-ray diffraction study on sodium germanate glasses and liquids did not yield any detectable change in the proportion of high-coordination Ge (Kamiya et al., 1986).

There are also a number of molecular dynamic simulation studies bearing on this problem. Molecular dynamic simulations of SiO_2 and its isostructural liquids (BeF_2 and GeO_2) indicate that the proportion of ^{15}Si decreases with decreasing temperature (Brawer, 1985). Another molecular dynamic study of titanium silicate glasses has shown that ^{47}Ti , ^{49}Ti , and ^{67}Ti coexist, but the proportions of Ti in different coordination states change with both quench rate and composition (Rosenthal and Garofalini, 1988). It is unclear, though, whether these computer simulations are directly applicable because they employ cooling rates that were more than ten orders faster than are obtainable in laboratory experiments. Nevertheless, the existing experimental results and computer simulations both suggest that the proportions of network-forming cations (Si, Ge, Al, B, Ti, etc.) in different coordination states are dependent on temperature, and this temperature dependence may vary with bulk composition. There is perhaps no general trend for all compositions as to whether lower temperature favors the higher coordination states for network-forming cations, or vice versa.

Mechanisms for Si speciation and coordination changes

Speciation disproportionation. Increased Q speciation disproportionation with pressure is indicated by both NMR and Raman spectra, at least for $\text{Na}_2\text{Si}_2\text{O}_7$ glasses. This type of pressure effect was first proposed to account for changes in the Raman spectra of quenched $\text{K}_2\text{Si}_4\text{O}_9$ glasses with pressure (Dickinson and Scarfe, 1985). As discussed in Xue et al. (1989), similar change also occurs

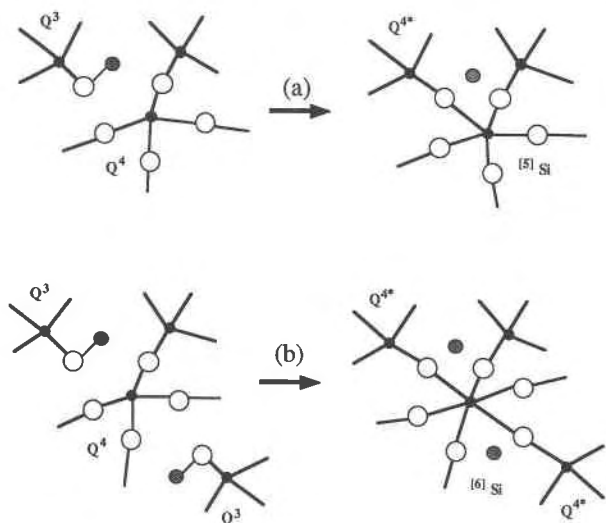
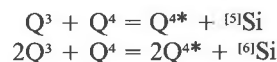


Fig. 13. Schematic model showing the formation of ¹⁵Si and ¹⁶Si in silicate melts by reactions (a) $Q^3 + Q^4 = Q^{4*} + {}^{15}\text{Si}$ and (b) $2Q^3 + Q^4 = 2Q^{4*} + {}^{16}\text{Si}$. Solid circles represent Si atoms, open circles are O atoms, and shaded circles are Na atoms.

when the type of network modifying cation is replaced by a smaller cation, e.g., Li^+ . This compositional effect has been well characterized by both molecular orbital calculations and spectroscopy and can be interpreted as being caused by stronger interaction with bridging O by a higher field strength cation (with larger Z/r^2 : Z = charge; r = ionic radii) (e.g., de Jong and Brown, 1980; McMillan and Piriou, 1983; Murdoch et al., 1985). Our results are thus consistent with the effect of pressure reducing the size of the sites for network-modifying cations, which is expected because it is easier to compress the network structure by reducing the Si-O-Si angle and NaO_n polyhedra than compressing the SiO_4 tetrahedra (cf. Hazen, 1985). This is also consistent with the molecular dynamic simulation result that the diffusion rate of Na decreases with pressure in silicate melts of similar compositions (Angell et al., 1982).

Transformation of Si coordination. The degree of polymerization of silicate melts and glasses plays a major role in controlling their structure and physical properties at 1 atm (cf. Mysen, 1987). The structure of partially depolymerized melts, such as alkali silicate melts studied here, in particular, contrasts with that of SiO_2 or other tectosilicate melts in that they contain nonbridging O atoms at 1 atm. Here we propose that this feature is the most important factor in determining the mechanism of the change of Si coordination with pressure. Conversion of the nonbridging O atoms to bridging O atoms is a likely mechanism for the formation of high-coordination Si species in partially depolymerized melts. This is because it does not involve Si-O bond breaking or formation of three-coordinated O (³O), but does create the extra Si-O bonds needed for the formation of high-coordination Si species. Whether high-coordination Si species are formed

at a given pressure may be dictated by the competition for O between Si and network modifying cations. In this discussion, we assume a role of ¹⁵Si and ¹⁶Si as network formers rather than network modifiers. As a consequence, any O atom linked directly to two Si atoms (¹⁴Si, ¹⁵Si, or ¹⁶Si) is regarded as a bridging O atom. This assumption does not necessarily imply that the melt viscosity should increase when high-coordination Si species appear because it is also related to the strength of Si-O bonds. A schematic structural model is presented in Figure 13 to explain this mechanism in the studied systems, which can be expressed by the following simple reactions:



where Q^3 and Q^4 are the dominant structural units in the low pressure glasses of the systems studied and Q^{4*} is a SiO_4 species with three ¹⁴Si and one ¹⁶Si (or ¹⁵Si) neighbors. We have no intention here to quantify our model, and thus do not rule out the possibility of forming SiO_4 species with two neighbors of ¹⁶Si (or ¹⁵Si) or even sharing edges with the latter. The connectivity of ¹⁴Si and ¹⁶Si (or ¹⁵Si) possibly depend on the bulk NBO/T and the abundances of high coordination Si in the system. When the abundances of ¹⁵Si and ¹⁶Si are low, ¹⁴Si may share at most one O with ¹⁶Si (or ¹⁵Si) and the latter are likely to be isolated from each other with up to 6 (or 5) ¹⁴Si neighbors (depending on the bulk NBO/T). At higher abundances of these species, a large percentage of ¹⁴Si may share two corners or even edges with ¹⁶Si (or ¹⁵Si) neighbors. These differences cannot be readily resolved, however, by the NMR, Raman, or infrared spectra.

The general mechanism of forming high-coordination species at the expense of nonbridging O atoms has been previously recognized for Ge coordinations in alkali germanate glasses (and melts) at 1 atm by examining the proportions of high coordination species and the proportion of nonbridging O atoms across the $R_2\text{Ge}_2\text{O}_5\text{-SiO}_2$ (where $R = \text{Li, Na, K, } \dots$) binaries (cf. Ueno et al., 1983). Our observed change in the proportions of high coordination Si species across the $\text{Na}_2\text{Si}_2\text{O}_5\text{-SiO}_2$ binaries at 6 GPa (the only complete data set we have so far) are consistent with those results: within the range of $\text{Na}_2\text{Si}_2\text{O}_5\text{-SiO}_2$, the proportions of ¹⁵Si and ¹⁶Si in the glasses at 6 GPa are highest near the tetrasilicate composition, and decrease toward SiO_2 , as well as toward $\text{Na}_2\text{Si}_2\text{O}_5$. Various spectroscopic studies (e.g., X-ray diffraction, neutron scattering, Raman, and infrared) suggest that alkali germanate glasses ($R_2\text{Ge}_2\text{O}_5\text{-GeO}_2$) at 1 atm contain both ¹⁴Ge and ¹⁶Ge species and show a similar pattern across the compositional range: the average Ge coordination displays a maximum near $R_2\text{Ge}_4\text{O}_9$ composition and decreases toward both pure GeO_2 and $R_2\text{Ge}_2\text{O}_5$ (cf. Ueno et al., 1983). This change in Ge coordination is related to the anomalous behavior of various physical properties (e.g., refractive index, density) and is called the german-

ate anomaly. Neutron scattering experiments (Ueno et al., 1983) support our suggested mechanism: the increase in average Ge coordination from GeO_2 to $R_2\text{Ge}_4\text{O}_9$ is accompanied by the formation of few, if any, nonbridging O atoms. At higher $R_2\text{O}$ contents, the decreasing proportion of high coordination Ge corresponds to a rapid increase in the number of nonbridging O atoms, suggesting an increased importance for a competing process such as destabilization of bridging O atoms by the greater proportion of network modifiers. Similar changes have also been observed for B coordinations in alkali borate glasses at 1 atm by ^{11}B NMR (Bray and O'Keefe, 1963; Jellison et al., 1978) and a similar mechanism was recognized based on molecular dynamic simulations (Xu et al., 1988). This compositional trend is also observable in $\text{Na}_2\text{O-SiO}_2\text{-P}_2\text{O}_5$ glasses at 1 atm for Si coordinations (see ^{29}Si NMR data in Weeding et al., 1985; Dupree et al., 1987, 1989). It is likely that this mechanism governs the formation of high-coordination Si (and analogues) for partially depolymerized melts and glasses. Further study of O coordinations in high-pressure alkali silicate glasses by ^{17}O NMR is in progress to test this model.

A similar mechanism may govern high-pressure phase transitions involving Si coordination changes in crystalline nontectosilicate systems (in which the low pressure phases contain nonbridging O atoms). Several high-pressure nontectosilicate and 1 atm germanate phases have been found to have a fully polymerized structure (containing no nonbridging O atoms) in which ^{14}Si and ^{16}Si (or Ge analogues) coexist (e.g., wadeite- $\text{K}_2\text{Si}_4\text{O}_9$, Kinomura et al., 1975; $\text{K}_2\text{Ge}_4\text{O}_9$, $\text{K}_2\text{Ge}_8\text{O}_{17}$, cf. Ueno et al., 1983). Interestingly, high-coordination Si first appears at similar pressures in the melts and crystalline phases for each of the three alkali silicate compositions studied (Kanzaki et al., 1989). A possible explanation is that conversion of nonbridging O atoms does not involve Si-O bond breaking; thus this transformation is less dependent on the longer-range order of the structure.

In summary, we have shown that the increase in Si coordination as a result of the consumption of nonbridging O atoms in partially depolymerized systems is more likely than simple reduction of Si-O-Si bond angles, as proposed by Stolper and Ahrens (1987). The latter may not be a dominant factor for the increased Si coordinations in partially depolymerized melts, but could be important for tectosilicate melts (e.g., SiO_2 and $\text{NaAlSi}_3\text{O}_8$), in which no nonbridging O atoms are available. When all the nonbridging O atoms are consumed, further transformation of ^{14}Si to higher coordinations would require a different mechanism, perhaps one similar to that for tectosilicates. In this case the model proposed by Stolper and Ahrens (1987) involving the reduction of Si-O-Si angles and development of ^{13}O may apply. Formation of high-coordination Si by this mechanism may be more difficult because it involves significant Si-O bond reconstruction and the resultant ^{13}O species have high energy. Possibly for the same reason, transformation of Si (or its analogues) to high coordinations in tectosilicate melts has

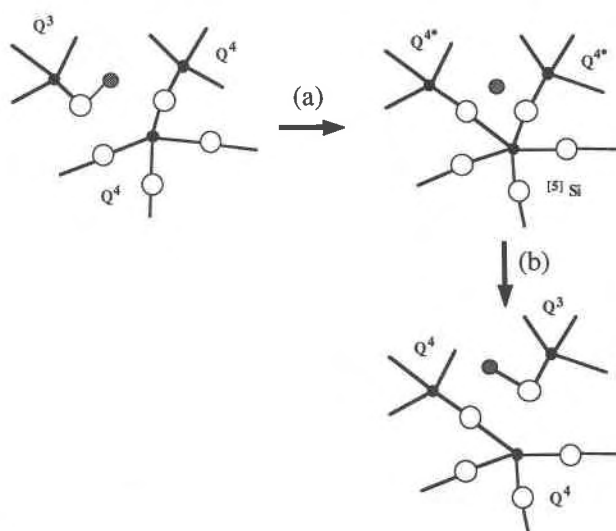


Fig. 14. Schematic model showing the diffusion and viscous flow processes via an intermediate state of ^{15}Si . The process (a) represents the formation of ^{15}Si species as in Figure 13a and process (b) shows the transformation of the structure to a ^{14}Si state with a configuration different from the initial state. Symbols as Figure 13.

been observed to take place at much higher pressure in glasses and melts than in corresponding crystalline phases (e.g., $\text{NaAlSi}_3\text{O}_8$ and GeO_2) (Ohtani et al., 1985; Fleet et al., 1984).

Transport and thermodynamic properties

The formation of short-lived sites involving five-coordinated cations (e.g., ^{15}Si) and three-coordinated anions (e.g., ^{13}O) has been given a key role in viscous flow in network liquids (tectosilicates and their structural analogues) based on molecular dynamic simulations (Brawer, 1985). As discussed earlier, formation of ^{15}Si in partially depolymerized melts and glasses may not be accompanied by formation of ^{13}O because high-coordination Si species can be created by converting nonbridging O atoms to bridging O atoms. The observed ^{15}Si in the systems reported on here survived relaxation during temperature quench and decompression and thus has a finite life time and represents a local free energy minimum that becomes deeper with increasing pressure (corresponding to an increase in the abundance of ^{15}Si). Such a high-coordination Si species may therefore play a role in viscous flow and in the reduction in viscosities observed at high pressures. A simple model similar to that in Liu et al. (1988) is presented in Figure 14 to explain this dynamic process as well as the formation of ^{15}Si in the alkali silicate melts at high pressures. In this model, a nonbridging O atom in Q^3 first approaches a neighboring Q^4 , resulting in a ^{15}Si species. This intermediate state could either return to the initial state or transform to a state of Q^3 and Q^4 with a different configuration. The latter is a process of Q species exchange as was envisioned from

NMR experiments by Liu et al. (1988), rather than diffusion of individual cations. The Q species exchange thus directly connects with viscous flow process (also see Stebbins and Farnan, 1989 and Farnan and Stebbins, 1990). Furthermore, we may speculate that ^{15}Si could also act as an intermediate state for the exchange reaction of ^{16}Si and ^{14}Si .

Another contribution to pressure-induced reduction of melt viscosity may be increased configurational entropy. The coexistence of all three coordination states as well as the greater distribution of Q species imply a larger configurational entropy, which is inversely related to melt viscosity (Adam and Gibbs, 1965; Richet, 1984; Richet et al., 1986). This factor may well act along with the role of ^{15}Si for the enhancement of diffusion and viscous flow in the melts at high pressures.

Finally, Q speciation disproportionation and Si coordination changes may also be accompanied by changes in the SiO_2 activity relative to a standard state with tetrahedrally coordinated Si because the latter has been shown by previous studies to be related to the abundance of Q^4 (e.g., Stebbins, 1988).

SUMMARY AND CONCLUSIONS

We observed several types of structural changes in alkali silicate and silica glasses quenched from liquids with increasing pressure. The most significant of these changes is the occurrence of five- and six-coordinated Si in the melts at high pressures. The ^{15}Si and ^{16}Si species appear simultaneously with pressure, but have different abundances for each composition. The formation of high coordination Si is gradual as expected because of the variety of structural units in silicate melts and may involve conversion of nonbridging O atoms to bridging O atoms rather than formation of three-coordinated O atoms. We also observed changes in the tetrahedral structure, including development of new species with ^{15}Si or ^{16}Si neighbors, increased Q speciation disproportionation with pressure, and reduction in the mean Si-O-Si angles around Q^3 and Q^4 sites. These changes may all, to some extent, contribute to compression of the liquid, and may also play a role in the melt viscosity and thermodynamic properties at high pressures.

ACKNOWLEDGMENTS

We would like to thank I. Farnan for help, and R.W. Luth, R.J. Kirkpatrick, and an anonymous reviewer for comments. X.X. acknowledges the late C.M. Scarfe for his inspiration of her interests in silicate melts. M.K. thanks E. Takahashi and E. Ito for their essential contribution to the design and construction of the 2000 ton multianvil press installed at the University of Alberta. This work was supported by the Natural Sciences and Engineering Research Council of Canada grants SMI-105, CII0006947, and OGP0008394 to C.M. Scarfe, U.S. National Science Foundation grants EAR-8707175 and EAR-8553024 to J.F.S., and EAR-8616990 to P.F.M.

REFERENCES CITED

Adam, G., and Gibbs, J.H. (1965) On the temperature dependence of cooperative relaxation properties in glass-forming liquids. *Journal of Chemical Physics*, 43, 139–146.

- Andersson, S., and Wadsley, A.D. (1960) Five co-ordinated titanium in $\text{K}_2\text{Ti}_2\text{O}_7$. *Nature*, 187, 499–500.
- Angell, A.C., Cheeseman, P., and Tamaddon, S. (1982) Pressure enhancement of ion mobilities in liquid silicates from computer simulation studies to 800 kilobars. *Science*, 218, 885–887.
- (1983) Water-like transport property anomalies in liquid silicates investigated at high T and P by computer simulation techniques. *Bulletin de Minéralogie*, 106, 87–97.
- Angell, C.A., Cheeseman, P.A., and Kadiyala, R.R. (1987) Diffusivity and thermodynamic properties of diopside and jadeite melts by computer simulation studies. *Chemical Geology*, 62, 83–92.
- Angell, C.A., Scamehorn, C.A., Phifer, C.C., Kadiyala, R.R., and Cheeseman, P.A. (1988) Ion dynamics studies of liquid and glassy silicates, and gas-in-liquid solutions. *Physics and Chemistry of Minerals*, 15, 221–227.
- Brandriss, M.E., and Stebbins, J.F. (1988) Effects of temperature on the structure of silicate liquids: ^{29}Si NMR results. *Geochimica et Cosmochimica Acta*, 52, 2659–2669.
- Brawer, S.A. (1985) A theory of the specific heat and viscosity of liquid SiO_2 and BeF_2 . In R.N. Shock, Ed., *Point defects in minerals*, p. 36–46. American Geophysical Union, Washington, DC.
- Brawer, S.A., and White, W.B. (1975) Raman spectroscopic investigation of the structure of silicate glasses. I. The binary alkali silicates. *Journal of Chemical Physics*, 63, 2421–2432.
- Bray, P.J., and O'Keefe, J.G. (1963) Nuclear magnetic resonance investigations of the structure of alkali borate glasses. *Physics and Chemistry of Glasses*, 4, 37–46.
- Burnham, C.W., and Buerger, M.J. (1961) Refinement of the crystal structure of andalusite. *Zeitschrift für Kristallographie*, 115, 269–290.
- Cella, J.A., Cargioli, J.D., and Williams, E.A. (1980) ^{29}Si NMR of five- and six-coordinate organosilicon complexes. *Journal of Organometallic Chemistry*, 186, 13–17.
- Crozier, D., and Douglas, R.W. (1965) Study of sodium silicate glasses in the infra-red by means of thin films. *Physics and Chemistry of Glasses*, 6, 240–245.
- de Jong, B.H.W.S., and Brown, G.E., Jr. (1980) Polymerization of silicate and aluminate tetrahedra in glasses, melts and aqueous solutions—II. The network modifying effects of Mg^{2+} , K^+ , Na^+ , Li^+ , H^+ , OH^- , F^- , Cl^- , H_2O , CO_2 , and H_3O^+ on silicate polymers. *Geochimica et Cosmochimica Acta*, 44, 1627–1642.
- Devine, R.A.B., Dupree, R., Farnan, I., and Capponi, J.J. (1987) Pressure-induced bond angle variation in amorphous SiO_2 . *Physical Review B*, 35, 2560–2562.
- Dickinson, J.E., Jr., and Scarfe, C.M. (1985) Pressure induced structural changes in $\text{K}_2\text{Si}_4\text{O}_9$ silicate melt. *Eos*, 66, 395.
- Dickinson, J.E., Jr., Scarfe, C.M., and McMillan, P. (1990) Physical properties and structure of $\text{K}_2\text{Si}_4\text{O}_9$ melt quenched from pressures up to 2.4 GPa. *Journal of Geophysical Research*, 95, 15675–15681.
- Domine, F., and Piriou, B. (1983) Study of sodium silicate melt and glass by infrared reflectance spectroscopy. *Journal of Non-Crystalline Solids*, 55, 125–130.
- Dowty, E. (1987) Vibrational interactions of tetrahedra in silicate glasses and crystals III. Calculations on simple sodium and lithium silicates, thortveitite and rankinite. *Physics and Chemistry of Minerals*, 14, 542–552.
- Dupree, R., Holland, D., McMillan, P.W., and Pettifer, R.F. (1984) The structure of soda-silica glasses: A MAS NMR study. *Journal of Non-Crystalline Solids*, 68, 399–410.
- Dupree, R., Holland, D., and Williams, D.S. (1986) The structure of binary alkali silicate glasses. *Journal of Non-Crystalline Solids*, 81, 185–200.
- Dupree, R., Holland, D., and Mortuza, M.G. (1987) Six-coordinated silicon in glasses. *Nature*, 328, 416–417.
- Dupree, R., Holland, D., Mortuza, M.G., Collins, J.A., and Lockyer, M.W.G. (1989) Magic angle spinning NMR of alkali phospho-aluminosilicate glasses. *Journal of Non-Crystalline Solids*, 112, 111–119.
- Engelhardt, G., and Radeglia, R. (1984) A semi-empirical quantum-chemical rationalization of the correlation between SiOSi angles and ^{29}Si NMR chemical shifts of silica polymorphs and framework aluminosilicates (zeolites). *Chemical Physics Letters*, 108, 271–274.
- Fay, V.E., Vollenkle, H., and Wittmann, A. (1973) Die kristallstruktur

- des kaliumoktagermanats, $K_2Ge_8O_{17}$. *Zeitschrift für Kristallographie*, 138, 439–448.
- Farnan, I., and Stebbins, J.F. (1990) A high temperature ^{29}Si investigation of solid and molten silicates. *Journal of the American Chemical Society*, 112, 32–39.
- Furukawa, T., Fox, K.E. and White, W.B. (1981) Raman spectroscopic investigation of the structure of silicate glasses. III. Raman intensities and structural units in sodium silicate glasses. *Journal of Chemical Physics*, 75, 3226–3237.
- Fleet, M.E., Herzberg, C.T., Henderson, G.S., Crozier, E.D., Osborne, M.D., and Scarfe, C.M. (1984) Coordination of Fe, Ga and Ge in high pressure glasses by Mossbauer, Raman and X-ray absorption spectroscopy, and geological implications. *Geochimica et Cosmochimica Acta*, 48, 1455–1466.
- Geisinger, K.L., Ross, N.L., McMillan, P., and Navrotsky, A. (1987) $K_2Si_4O_8$: Energetics and vibrational spectra of glass, sheet silicate, and wadeite-type phases. *American Mineralogist*, 72, 984–994.
- Gibbs, J.H., and DiMarzio, E.A. (1958) Nature of the glass transition and the glassy state. *Journal of Chemical Physics*, 28, 373–383.
- Grimmer, A., and Muller, W. (1986) ^{29}Si -MAS-NMR-Untersuchungen an binären kaliumsilicatgläsern Ein Beitrag zur Interpretationskontroverse. *Monatshefte für Chemie*, 117, 799–803.
- Gupta, P.K., Lui, M.L., and Bray, P.J. (1985) Boron coordination in rapidly cooled and in annealed aluminum borosilicate glass fibers. *Journal of the American Ceramic Society*, 68, C82.
- Hazen, R.M. (1985) Comparative crystal chemistry and the polyhedral approach. In *Mineralogical Society of America Reviews in Mineralogy*, 14, 317–346.
- Hemley, R.J., Mao, H.K., Bell, P.M., and Mysen, B.O. (1986) Raman spectroscopy of SiO_2 glass at high pressure. *Physical Review Letters*, 57, 747–750.
- Hochella, M.F., Jr., and Brown, G.E. (1985) The structure of albite and jadeite composition glasses quenched from high pressure. *Geochimica et Cosmochimica Acta*, 49, 1137–1142.
- Itie, J.P., Polian, A., Calas, G., Petiau, J., Fontaine, A., and Tolentino, H. (1989) Pressure-induced coordination changes in crystalline and vitreous GeO_2 . *Physical Review Letters*, 63, 398–401.
- Ito, E., Takahashi, E., and Matsui, Y. (1984) The mineralogy and chemistry of the lower mantle: An implication of ultra-high pressure phase relations in the system MgO - FeO - SiO_2 . *Earth and Planetary Science Letters*, 67, 238–248.
- Jellison, G.E., Feller, S.A., and Bray, P.J. (1978) A re-examination of the fraction of 4-coordinated boron atoms in the lithium borate glass system. *Physics and Chemistry of Glasses*, 19, 52–53.
- Kamiya, K., Yoko, T., Itoh, Y., and Sakka, S. (1986) X-ray diffraction study of Na_2O - GeO_2 melts. *Journal of Non-Crystalline Solids*, 79, 285–294.
- Kanzaki, M. (1991) Melting of silica up to 7 GPa. *Journal of the American Ceramic Society*, in press.
- Kanzaki, M., Xue, X., and Stebbins, J.F. (1989) High pressure phase relations in $Na_2Si_2O_5$, $Na_2Si_4O_9$ and $K_2Si_4O_9$ up to 12 GPa. *Eos*, 70, 1418.
- Kinomura, N., Kume, S., and Koizumi, M. (1975) Synthesis of $K_2Si_4O_9$ with silicon in 4- and 6-coordination. *Mineralogical Magazine*, 40, 401–404.
- Kirkpatrick, R.J. (1988) MAS NMR spectroscopy of minerals and glasses. In *Mineralogical Society of America Reviews in Mineralogy*, 18, 341–403.
- Litovitz, T.A. (1960) Liquid relaxation phenomena and the glass state. In V.N. Frechette, Ed., *Non-crystalline solids*, p. 252–268. Wiley, New York.
- Liu, L.-G., and Bassett, W.A. (1986) Elements, oxides, silicates; high-pressure phases with implications for the Earth's interior, 250 p. Oxford University Press, New York.
- Liu, S.-B., Stebbins, J.F., Schneider, E., and Pines, A. (1988) Diffusive motion in alkali silicate melts: An NMR study at high temperature. *Geochimica et Cosmochimica Acta*, 52, 527–538.
- Marsmann, H. (1981) Silicon-29 NMR. In P. Diehl, E. Fluck, and R. Kosfeld, Eds., *NMR basic principles and progress*, vol. 17, p. 65–235. Springer-Verlag, Berlin.
- Matson, D.W., Sharma, S.K., and Philpotts, J.A. (1983) The structure of high-silica alkali-silicate glasses. A Raman spectroscopic investigation. *Journal of Non-Crystalline Solids*, 58, 323–352.
- Matsui, Y., and Kawamura, K. (1980) Instantaneous structure of an $MgSiO_3$ melt simulated by molecular dynamics. *Nature*, 285, 648–649.
- (1984) Computer simulation of structures of silicate melts and glasses. In I. Sunagawa, Ed., *Materials science of the Earth's interior*, p. 3–23. Terra Scientific Publishing Company, Tokyo.
- Matsui, Y., Kawamura, K., and Syono, Y. (1982) Molecular dynamics calculations applied to silicate systems: Molten and vitreous $MgSiO_3$ and Mg_2SiO_4 under low and high pressures. In S. Akimoto and M.H. Manghnani, Eds., *Advances in earth and planetary sciences*, vol. 12, high pressure research in geophysics, p. 511–524. Reidel, Tokyo.
- McMillan, P. (1984) Structural studies of silicate glasses and melts—Applications and limitations of Raman spectroscopy. *American Mineralogist*, 69, 622–644.
- McMillan, P.F., and Piriou, B. (1983) Raman spectroscopic studies of silicate and related glass structure: A review. *Bulletin de Mineralogie*, 106, 57–75.
- McMillan, P.F., and Ross, N.L. (1987) Heat capacity calculations for Al_2O_3 , corundum and $MgSiO_3$, ilmenite. *Physics and Chemistry of Minerals*, 14, 225–234.
- McMillan, P., Piriou, B., and Couty, R. (1984) A Raman study of pressure-densified vitreous silica. *Journal of Chemical Physics*, 81, 4234–4236.
- McMillan, P., Akaogi, M., Ohtani, E., Williams, Q., Nieman, R., and Sato, R. (1989) Cation disorder in garnets along the $Mg_3Al_2Si_3O_{12}$ - $Mg_2Si_2O_7$ join: An infrared, Raman and NMR study. *Physics and Chemistry of Minerals*, 16, 428–435.
- Murdoch, J.B., Stebbins, J.F., and Carmichael, I.S.E. (1985) High-resolution ^{29}Si NMR study of silicate and aluminosilicate glasses: The effect of network-modifying cations. *American Mineralogist*, 70, 332–343.
- Mysen, B.O. (1987) Magmatic silicate melts: Relations between bulk composition, structure and properties. In B.O. Mysen, Ed., *Magmatic processes: Physicochemical principles*, p. 375–400. Geochemical Society Special Publication No. 1.
- (1988) *Structure and properties of silicate melts*. Elsevier, Amsterdam.
- Mysen, B.O., Virgo, D., Danckwerth, P., Seifert, F.A., and Kushiro, I. (1983) Influence of pressure on the structure of melts on the joins $NaAlO_2$ - SiO_2 , $CaAl_2O_4$ - SiO_2 , and $MgAl_2O_4$ - SiO_2 . *Neues Jahrbuch für Mineralogie Abhandlungen*, 147, 281–303.
- Oestrike, R., Yang, W.-H., Kirkpatrick, R.J., Hervig, R.L., Navrotsky, A., and Montez, B. (1987) High-resolution ^{23}Na , ^{27}Al , and ^{29}Si NMR spectroscopy of framework aluminosilicate glasses. *Geochimica et Cosmochimica Acta*, 51, 2199–2209.
- Ohtani, E., Taulelle, F., and Angell, A.C. (1985) Al^{3+} coordination changes in liquid aluminosilicates under pressure. *Nature*, 314, 78–81.
- Phillips, B.L., Kirkpatrick, R.J., and Hovis, G.L. (1988) ^{27}Al , ^{29}Si , and ^{23}Na MAS NMR study of an Al, Si ordered alkali feldspar solid solution series. *Physics and Chemistry of Minerals*, 16, 262–275.
- Richtet, P. (1984) Viscosity and configurational entropy of silicate melts. *Geochimica et Cosmochimica Acta*, 48, 471–483.
- Richtet, P., Robie, R.A., and Hemingway, B.S. (1986) Low-temperature heat capacity of diopside glass ($CaMgSi_2O_6$): A calorimetric test of the configurational-entropy theory applied to the viscosity of liquid silicates. *Geochimica et Cosmochimica Acta*, 50, 1521–1533.
- Risbud, S.H., Kirkpatrick, R.J., Tagliavere, A.P., and Montez, B. (1987) Solid-state NMR evidence of 4-, 5-, and 6-fold aluminum sites in roller-quenched SiO_2 - Al_2O_3 glasses. *Journal of American Ceramic Society*, 70, C-10–C-12.
- Rosenhauer, M., Scarfe, C.M., and Virgo, D. (1979) Pressure dependence of the glass transition temperature in glasses of diopside, albite, and sodium trisilicate composition. *Carnegie Institute of Washington Geophysical Lab Annual Report*, 78, 556–559.
- Rosenthal, A.B., and Garofalini, S.H. (1988) Molecular dynamics study of amorphous titanium silicate. *Journal of Non-Crystalline Solids*, 107, 65–72.
- Sanders, D.M., Person, W.B., and Hench, L.L. (1974) Quantitative analysis of glass structure with the use of infrared reflection spectra. *Applied Spectroscopy*, 28, 247–255.
- Sato, R.K., McMillan, P.F., Dupree, R., and Dennison, P. (1989) MAS

- NMR investigation of Al and Si coordination in aluminosilicate glasses. *Eos*, 70, 1374.
- Scarfe, C.M., Mysen, B.O., and Virgo, D. (1979) Changes in viscosity and density of sodium disilicate, sodium metasilicate, and diopside composition with pressure. *Carnegie Institute of Washington Year Book*, 78, 547–551.
- Schneider, E., Stebbins, J.F., and Pines, A. (1987) Speciation and local structure in alkali and alkaline earth silicate glasses: Constraints from Si-29 NMR spectroscopy. *Journal of Non-Crystalline Solids*, 89, 371–383.
- Simon, I., and McMahon, H.O. (1953) Study of some binary silicate glasses by means of reflection in infrared. *Journal of the American Ceramic Society*, 36, 160–164.
- Smith, J.V., and Blackwell, C.S. (1983) Nuclear magnetic resonance of silica polymorphs. *Nature*, 303, 223–225.
- Stebbins, J.F. (1987) Identification of multiple structural species in silicate glasses by ^{29}Si NMR. *Nature*, 330, 465–467.
- (1988) Effects of temperature and composition on silicate glass structure and dynamics: ^{29}Si NMR results. *Journal of Non-Crystalline Solids*, 106, 359–369.
- Stebbins, J.F., and Farnan, I. (1989) Nuclear magnetic resonance spectroscopy in the earth sciences: Structure and dynamics. *Science*, 245, 233–332.
- Stebbins, J.F., and Kanzaki, M. (1991) Local structure and chemical shifts for six-coordinated silicon in high-pressure mantle phases. *Science*, in press.
- Stebbins, J.F., and McMillan, P. (1989) Five- and six-coordinated Si in $\text{K}_2\text{Si}_2\text{O}_7$ liquid at 1.9 GPa and 1200 °C. *American Mineralogist*, 74, 965–968.
- Stebbins, J.F., and Sykes, D. (1990) The structure of $\text{NaAlSi}_3\text{O}_8$ liquid at high pressure: New constraints from NMR spectroscopy. *American Mineralogist*, 75, 943–946.
- Stolper, E.M., and Ahrens, T.J. (1987) On the nature of pressure-induced coordination changes in silicate melts and glasses. *Geophysical Research Letters*, 14, 1231–1233.
- Sweet, J.R., and White, W.B. (1969) Study of sodium silicate glasses and liquids by infrared reflectance spectroscopy. *Physics and Chemistry of Glasses*, 10, 246–251.
- Taylor, W.H. (1929) The structure of andalusite, Al_2SiO_5 . *Zeitschrift für Kristallographie*, 71, 205–218.
- Tossell, J.A. (1990) Calculation of NMR shieldings and other properties for three and five coordinate Si, three coordinate O and some siloxane and boroxol ring compounds. *Journal of Non-Crystalline Solids*, 120, 13–19.
- Tossell, J.A., and Lazeretti, P. (1986) Ab initio calculations of ^{29}Si chemical shifts for some gas phase and solid state silicon fluorides and oxides. *Journal of Chemical Physics*, 84, 369–374.
- Ueno, M., Misawa, M., and Suzuki, K. (1983) On the change in coordination of Ge atoms in $\text{Na}_2\text{O-GeO}_2$ glasses. *Physica*, 120B, 347–351.
- Weeding, T.L., de Jong, B.H.W.S., Veeman, W.S., and Aitken, B.G. (1985) Silicon coordination changes from 4-fold to 6-fold on devitrification of silicon phosphate glass. *Nature*, 318, 352–353.
- Williams, Q., and Jeanloz, R. (1988) Spectroscopic evidence for pressure-induced coordination and changes in silicate glasses and melts. *Science*, 239, 902–905.
- Williams, Q., Jeanloz, R., and McMillan, P. (1987) Vibrational spectrum of MgSiO_3 perovskite: Zero-pressure Raman and mid-infrared spectra to 27 GPa. *Journal of Geophysical Research*, 92, 8116–8128.
- Wolf, G., Durben, D.J., and McMillan, P. (1990) High-pressure Raman spectroscopic study of sodium tetrasilicate ($\text{Na}_2\text{Si}_4\text{O}_9$) glass. *Journal of Chemical Physics*, 93, 2280–2288.
- Xu, Q., Kawamura, K., and Yokokawa, T. (1988) Molecular dynamics calculations for boron oxide and sodium borate glasses. *Journal of Non-Crystalline Solids*, 104, 261–272.
- Xue, X., Stebbins, J.F., Kanzaki, M., and Trønnes, R.G. (1989) Silicon coordination and speciation changes in a silicate liquid at high pressures. *Science*, 245, 962–964.

MANUSCRIPT RECEIVED MARCH 19, 1990

MANUSCRIPT ACCEPTED NOVEMBER 14, 1990